5-14-2023

Past and Future Hydro-climatological Drivers of Summer Precipitation Variability in the Great Lakes Region in Coupled Model Intercomparison Project Phase 6 (CMIP6)

Tasmeem Jahan Meem
Syracuse University

Abstract

The Great Lakes Regions are the largest surface freshwater system on earth containing 20% of the global freshwater reserves and supply drinking water to 10% of the United States and 30% of the Canadian population. Nearly 25% of Canadian and 7% of American agricultural production are in the watershed. Trends and variability in precipitation over the Great Lakes basin has critical global and local implications for water resources management, which become especially problematic under climate change. Understanding how Great Lakes hydrometeorology will respond to anthropogenic climate change is complicated by the climatological complexity of the region. The Great Lakes basin spans over 1200 kilometers (about 745.65 mi) and straddles four different climate regions in two countries: the Midwestern and Eastern climate regions of the United States, and the Northeastern Forest and Laurentian Great Lakes climate regions of Canada. The atmospheric dynamics of hydroclimatic circulation vary across the Great Lakes basin. In the western Great Lakes, precipitation variability is strongly leveraged by the ENSO oscillation, in the eastern Great Lakes, precipitation variability is additionally impacted by circulation anomalies associated with the North Atlantic Hadley circulation. These atmospheric features will likely be impacted differently by climate change. Projecting pan-Great Lakes hydro-climatological shifts in the twenty-first century will require a diagnostic assessment of 1) how numerical climate models parameterize relationships between local circulation patterns and precipitation variability and 2) how these relationships will likely change under global warming. Currently, there is very little agreement in regional 21st century precipitation predictions between CMIP6 ensemble models. In this study, we evaluate precipitation simulations from 12 different general circulation models participating in CMIP6 that are representative of the full range of variability in numeric representation of North American climate. We quantify each model's accuracy in capturing historic seasonal wet and dry anomalies in the Great Lakes region. We then evaluate consistency between characteristic modes of anomalous hydroclimatic circulation in historical observations and model simulations. Based on the physical mechanism by which climate models simulate historical anomalous hydroclimatic circulation, and translate these circulation anomalies into precipitation anomalies, we identify a subset of 21st century climate model predictions which we believe to be most physically plausible. Implications for future hydroclimate are discussed.

Past and Future Hydro-climatological Drivers of Summer Precipitation Variability in the Great Lakes Region in Coupled Model Intercomparison Project Phase 6 (CMIP6)

By

Tasmeem Jahan Meem

B.S. Bangladesh University of Engineering and Technology, April 2019

Thesis

Submitted in partial fulfillment of the requirements for the degree of

Master of Science in Environmental Engineering

Syracuse University

May 2023

Acknowledgement

I would like to thank my family for always being my source of inspiration and encouragement. I would like to express my gratitude to my advisor Dr. Liz Carter for her constant support and guidance. She has been a great mentor for me who made my research journey a lot easier. Thanks to all my committee members Dr. Cliff Ian Davidson, Dr. Tripti Bhattacharya, Dr. Stephen B Shaw for their constructive feedbacks and suggestions in the process. Thanks to all the members of Climate Hazards Research Team Syracuse (CHaRTS) for their help. Last but not the least thanks to the department of Civil and Environmental Engineering, specially Nick Clark for all his prompt help naviagting all the official procedures.

Contents

List of Illustrative Materials

List of Tables

Section 1: Introduction

The Laurentian Great Lakes contain 20% of the world's surface freshwater, making them the largest surface freshwater system on earth. The Great Lakes supply drinking water to 8% of the United States and 30% of the Canadian population. According to the United States of Environmental Protection Agency (EPA), nearly 25% of Canadian agricultural production and 7% of American agricultural production occurs in the Great Lakes watershed. The Great Lakes surface water system, including the Saint Lawrence River, are essential inland navigation routes for the shipping industry. According to the Great Lakes St. Since 1959, over $375 billion in commodities have traveled through the Great Lakes seaway on transport to or from the United States and Canada. The management of the Great Lakes system involves international coordination between the United States and Canada by way of the International Joint Commission, as well as state and local governments across eight US states and two Canadian provinces. With so many stakeholders involved, and so much at stake, accurate information about current and future hydrologic conditions in the Great Lakes basin is essential to the coordination of successful human enterprise across North America.

Seager, Naik, and Vecchi (2010) demonstrate that global warming will modify local hydrologic variability both thermodynamically and dynamically, and that the fidelity of characterization of both mechanisms must be considered when evaluating the realism of local hydrologic predictions under climate change (Seager and Hoerling 2014; Seager et al. 2014). Thermodynamically, warmer air temperatures expected under global warming will have higher saturation vapor pressures, meaning that the maximum mass of water that can be retained by an atmospheric column increases as the temperature of that atmospheric column increases. The quantification of this feature comes from the Clausius Clapeyron equation. As average air temperatures increase under climate change, the maximum mass of water that can be in the atmosphere will increase as well, by about 7% for every 1^{o}C in temperature increase. Temperature-modulated increases in saturation vapor pressure will be associated with both an increase in precipitation rates (increased in the total mass and intensity of precipitation delivered during convection) and evaporation rates (an increase in the humidity gradient between moist land surfaces and warm dry air will increase rates of terrestrial drying). Often called "wet gets wetter, dry gets drier," thermodynamic intensification of the hydrologic cycle under global warming is expected to increase the net moisture supply in humid climates and increase the net aridity in arid climates (K. E. Trenberth 2011). Dynamically, the spatial distribution of humid and arid climates is determined by stable patterns in global atmospheric circulation. Atmospheric currents route moisture-enriched air from ocean basins over terrestrial landmasses, determining the spatial distribution of arid and humid landscapes at the continental scale (Gimeno et al. 2010). Atmospheric circulation patterns are complex, scale-dependent functions of earth's axial rotation, earth's orbit around the sun, thermal gradients in the oceans (which are modified by oceanic circulation), thermal gradients between land-sea interfaces, diabatic heating/cooling associated with internal atmospheric processes, and local landscape forcings such as land cover, elevation, and the presence of freshwater bodies. Dynamical shifts in hydroclimatology, that occur when increasing air temperatures modify large-scale atmospheric circulation patterns by way of modified thermal and osmotic gradients within oceans and across land masses, are projected to shift the geographic and seasonal distribution of terrestrial moisture supply. Taken in tandem, thermodynamic and dynamic shifts in hydroclimatology are expected to shift both the intensity of precipitation and evapotranspiration, and the space-time distribution of humidity and aridity across continental landmasses.

There is broad consensus on the impact of thermodynamic intensification of the hydrologic cycle across different general circulation models. An increase in temperature causes the atmosphere to have a greater capacity to hold water vapor, i.e., it increases the specific humidity exponentially with temperature. This moisture availability will result in an increase in the intensity of precipitation even though the average global precipitation will be constrained by the energy availability (Allen and Ingram 2002). Across all latitude bands the extreme precipitation sensitivity to temperature is found to be positive albeit with different magnitude (O'Gorman 2015, Pfahl, O'Gorman, and Fischer 2017) The increase in intensity also can be explained by the difference between larger increase in moisture and a relatively smaller increase in total precipitation change (K. E. Trenberth 2011;). There is substantial variability in how GCMs represent dynamic hydrological shifts, resulting in substantial regional variability between model projections. Variability in characterization of regional dynamic hydrologic change dominates the total uncertainty in multi-model ensemble forecasts of precipitation under climate change (Pfahl, O'Gorman, and Fischer 2017). The accuracy of regional precipitation forecasts under different global warming scenarios is therefore dependent on the physical realism of how these global models map regional precipitation anomalies to anomalies in global hydroclimatic circulation.

1.1 Dynamic drivers of precipitation variability in the Great Lakes Region

The primary moisture sources for the Great Lakes basin vary spatially and seasonally, with the majority of moisture delivered as precipitation to the basin originating from the subpolar Pacific Ocean in winter months, and from the subtropical Atlantic and Gulf of Mexico in summer months (Carter et al. 2021). The Great Lakes basin spans over 1200 kilometers and straddles four climate regions in two countries: the Midwestern and Eastern climate regions of the United States, and the Northeastern Forest and Laurentian Great Lakes climate regions of Canada. Across the Great Lakes basin, the driving hydroclimatic circulation varies spatially. In the western Great Lakes, winter precipitation is generally sourced from the subpolar Atlantic by way of the polar Jet Stream (Rodionov 1994). The zonal and meridional intensity of the jet stream have strong control over precipitation dynamics in the region is strongly leveraged by the El Nino Southern Oscillation, with La Nina events associated with enhanced meridional activity in the jet stream and strong moist anomalies in the Northern United States and Canada. Under climate change, both El Nino and La Nina events are expected to increase in frequency and intensity, with an expected westward migration in La Nina-associated wintertime moist anomalies in the upper latitudes of North America (Cai et al. 2014). This may be associated with increased interannual variability in wintertime precipitation, with a slight decline in the mean precipitation in the Great Lakes region.

In the eastern Great Lakes, particularly in the warm season, precipitation variability is additionally impacted by circulation anomalies associated with the North Atlantic subtropical high (NASH, also called the Azores High), which is a seasonally intensifying manifestation of the global Hadley circulation (Li et al. 2010). Longitudinal thermal gradients associated with warm-season land-sea thermal contrasts in the Eastern and Western Atlantic basin cause the NASH to migrate westward during spring months, deflecting a current of moist air from the subtropical Atlantic into the continental interior, where it is convectively recycled through the eastern upper mid-Latitudes during summer months. Westerly anomalies in the NASH are associated with moist anomalies in the Southeastern US and Midwestern US. Under climate change, thermodynamically enhanced land-sea thermal contrasts are anticipated to be associated with a westward shift in the

NASH at peak expansion, suggesting an increase in warm season precipitation sourced from the subtropical Atlantic.

1.2 Historical and future impacts of climate change on Great Lakes hydroclimatology

Understanding how Great Lakes hydrometeorology has and will respond to shifts in regional circulation associated with climate change is complicated by the hydroclimatological complexity of the region. In the past several decades, the research community has identified substantial, complex evidence of hydrologic non-stationarity associated with anthropogenic climate change, as well as human development and lake level management. In line with expectations for thermodynamic hydrologic intensification under global warming, increases in both evapotranspiration and precipitation (Held and Soden 2006) have been observed in the recent hydrologic record, leading to increased variability in lake levels across the Great Lakes.

Current climate models predict an increase in total precipitation but a drier summer in the Great Lakes region because of the extension of droughts in south-western USA to more northward and eastwards (Richard Peltier et al. 2018). The droughts decrease the surface evaporation in the south-west, which decreases the amount of recycled precipitation in the Great Lakes basin. There are also differences between how mean precipitation will change and how extreme precipitation will be changing. The change in mean precipitation is constrained by radiative cooling (Pendergrass and Hartmann 2014) but the main driver of changes in extreme precipitation is moisture divergence (Kevin E. Trenberth 1999). But there is little agreement among the models in characterizing the precipitation patterns and seasonality. Models that show a dry/wet bias in their historic projections tend to continue these biases in their future projections too (Minallah and Steiner 2021b). These uncertainties in projections mainly stem from the lack of lake – atmospheric climate process parameterizations in these models. Very few models represent lakes as dynamic lakes in their simulations, most models represent lakes as a static water body component of land surface or oceans, some of them do not simulate Great Lakes at all. Even the models who simulate dynamic lakes do not do a very good job in capturing lake dynamics because of their very coarse spatial resolution (Briley et al., 2021).

1.3 Study Objectives

Given notable lack of agreements between numerical models in historical and future precipitation forecasts for the Great Lakes region, the goal of this analysis is to identify a subset of CMIP6 contributing model(s) which provide the most realistic depiction of dynamic drivers of Great Lakes historical precipitation variability for operational use. We define the suitability of contributing models in two ways: prediction accuracy (how accurate are historical precipitation predictions) and mechanistic accuracy (how accurately does the model identify anomalies in regional hydroclimatic circulation associated with climate change). To evaluate prediction accuracy, we compare historical predictions of five indices of precipitation anomalies with observations. To evaluate mechanistic accuracy, we evaluate how well models capture characteristic anomalies in hydroclimatic circulation. We conclude with guidance on model selection for regional water resources managers, as well as advice for the global modeling community on broadly how to increase fidelity of models in this critical freshwater region.

1.4 Study Area

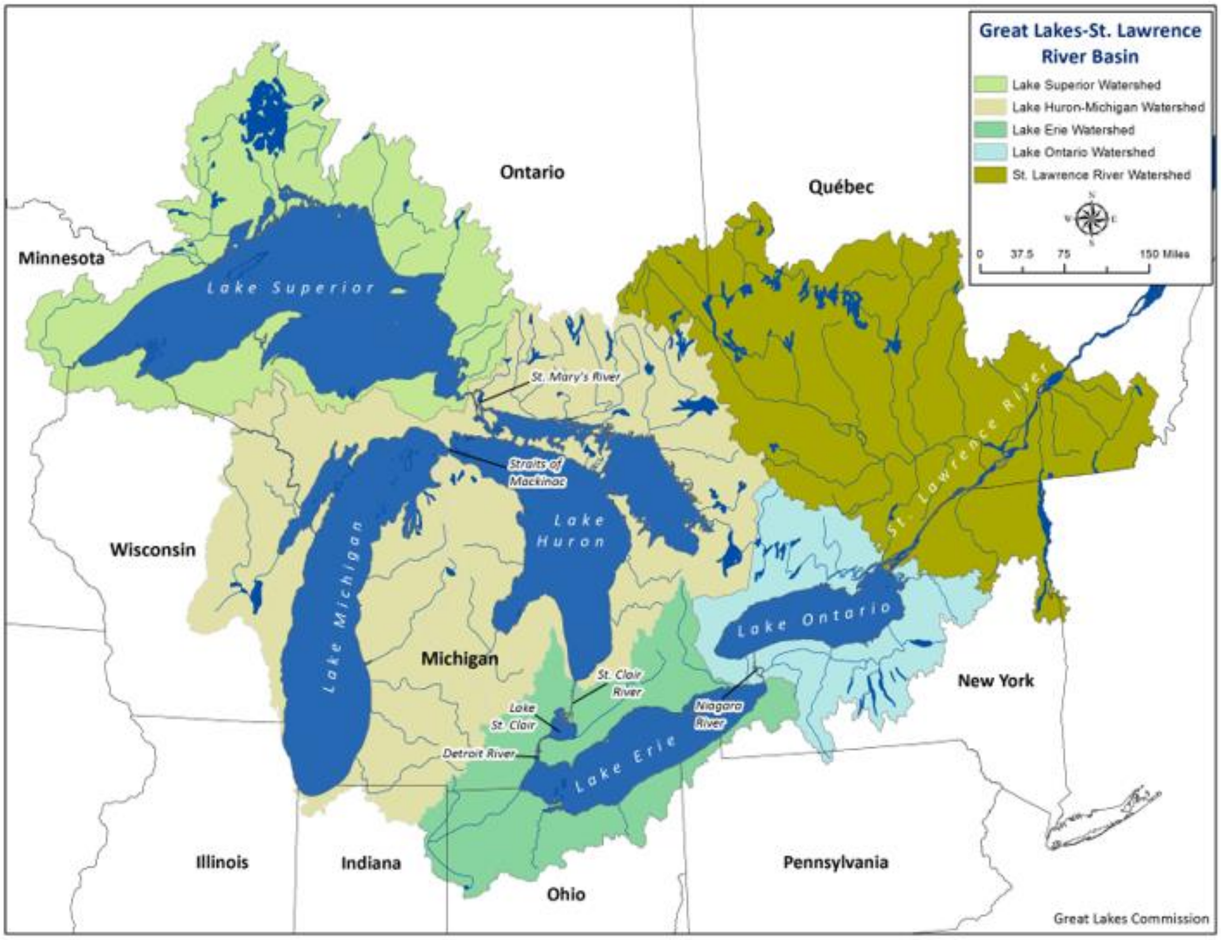

Figure 01: Great Lakes Basin Watershed Region

Section 2: Methods overview

2.1 Data:

2.1.1 Observed Data:

For historical precipitation we here use CPC Global Unified Gauge Based Analysis of Precipitation, a product of CPC Unified Precipitation Project that is underway at NOAA Climate Prediction Center (CPC). This daily dataset is available from 1979-present with a grid resolution of $0.5^0 \times 0.5^0$. This dataset is a gauge adjusted global precipitation dataset (Chen et al. 2008).

One challenge in choosing a precipitation dataset was to find a global dataset which covers a reasonable number of years. A global gridded dataset or a dataset that covers both Canada and contiguous US was needed to avoid any discrepancies in the precipitation data across international boundaries in the Great Lakes region. These discrepancies often can be found in using gauge precipitation products as the gauges in this area are managed by two different organizations.

2.1.2Coupled Model Intercomparison Project 6 (CMIP6)

The Coupled Model Intercomparison Project has undergone several phases since its inception in early 1990's. Each phase builds upon the success and limitations of previous phases and aims to have a better understanding of the earth's climate system. The latest phase, CMIP6, involves 42 modeling groups from around the world and produced a wealth of outputs that are being used to make informed decisions about climate policy and further research in the earth's climate system (Eyring et al., 2016). Many models participating in coupled model intercomparison projects (CMIPs) will share common theoretical or empirical assumptions, evolve from common code banks, or be developed at individual institutions. These common "genealogies" between models represent potential sources of non-independence in models that can be difficult to assess and can bias both projections and estimates of uncertainty when working with ensemble means (Steinschneider et al. 2015). To avoid functional redundancy between models, we selected twelve models that span the full range of grid resolution, equilibrium climate sensitivity, and regional transient climate representation among CMIP6 member models (Mahony et al. 2022; T. Wang et al. 2016). The 12 models used in this study is listed in the table below:

Table 1: Description of 12 CMIP6 models used.

Model Name	Institute	Latitude	Longitude	Names Used in Paper	Reference
ACCESS-ESM1-5	Commonwealth Scientific & Industrial Research Organisation	1.25^{0}	1.875^{0}	access	*Ziehn et al (2019)*
BCC-CSM2	Beijing Climate Center	1.25^{0}	1.875^{0}	bcc	*Wu et al (2018)*
CanESM5	Canadian Centre for Climate Modelling and Analysis	2.789327^{0}	2.8125^{0}	can_esm	*Swart et al(2019)*
CNRM-ESM2-1	Centre National de Recherches Météorologiques	1.400437^{0}	1.40625^{0}	cnrm_esm	*Seferian(2018)*
EC-Earth3	EC-Earth Consortium (EC-Earth)	0.7016692^{0}	0.703125^{0}	ec_earth	*EC-Earth Consortium (EC-Earth) (2019)*
GFDL-ESM4	Geophysical Fluid Dynamics Laboratory/NOAA	1^{0}	1.25^{0}	gfdl	*Krasting et al(2018)*
INM-CM5-0	Institute of Numerical Mathematics	1.5^{0}	2^{0}	inm	*Volodin et al (2019)*
IPSL-CM6A-LR	Institut Pierre-Simon Laplace	1.267606^{0}	2.5^{0}	ipsl	*Boucher et al(2018)*

MIROC-ES2L	Japan Agency for Marine-Earth Science and Technology	2.789327^0	2.8125^0	miroc	*Hajima et al(2019)*
MPI-ESM-1-2-HAM	Max-Planck-Institute fuer Meteorologie	1.864677^0	1.875^0	mpi	*Neubauer et al (2019)*
MRI-ESM2-0	Meteorological Research Institute	1.1125^0	1.1125^0	mri	*Youkimoto et al(2019)*

2.1.3 Historical CMIP6 simulations:

Historic (1850-2014) simulations are included in CMIP6 runs to allow comparison of tracking of past and future trends and changes in climate against change in external conditions independent from model error and bias. Historical simulations run are based on historical data of greenhouse gas emissions and concentrations, global gridded land-use forcing data sets, solar forcing, stratospheric aerosols (volcanos), Atmospheric Model Intercomparison Project (AMIP), sea surface temperatures (SSTs) and sea ice concentrations (SICs) (Eyring et al. 2016). We utilize historical precipitation data from all twelve models to assess overall prediction accuracy Geopotential height (z) anomalies from the five most accurate models were calculated from monthly height data in each model's historical simulation. These z anomalies are used to assess mechanistic fidelity when characterizing the hydroclimatic dynamics in the Great Lakes region.

2.1.4 Geopotential Height Data:

Historical geopotential height (z) data was obtained from the NCAR/NCEP reanalysis monthly dataset which has a resolution $2.5^0 \times 2.5^0$. This dataset covers the timeline from 1948 to 2017(Kalnay et al.1996). The extent was chosen from -7.5^0 to 90^0 in latitude and 182^0 to 360^0 in longitude. An average of summer height anomalies was calculated from this dataset. Height anomalies from the five chosen models were calculated from monthly height data in each model's historical simulation. These height simulations are in the same resolution as their precipitation simulations.

2.2 Historical model accuracy:

2.2.1 Precipitation data processing:

Basin wide daily precipitation is extracted for each of the five Great Lakes basins (Lake Huron, Lake Erie, Lake Michigan, Lake Ontario, Lake Superior) from both the historical CPC and CMIP6 member datasets. To evaluate bias in the climate models, the yearly total precipitation (1979-2014) and monthly average precipitation (1979-2014) are compared to the same values in the CPC dataset. The monthly average precipitation was compared using a nonparametric Wilcoxon test (alpha = 0.05) (Rey et al., 2011)

2.2.2 Precipitation Indices

Daily precipitation data for each grid point of the five Great Lakes were processed into five precipitation indices to capture dry anomalies (Cumulative Dry Days), moist anomalies (Cumulative Wet Days, Total Precipitation) and extreme precipitation anomalies (Extreme Precipitation Days, Maximum Daily Precipitation) (Table 2) (Zhang et al., 2011). All the indices were calculated for summer season i.e., June, July, and August.

Table 2: List of Precipitation Indices Calculated for both Historical Time Period and Future

Index	Definition	Unit
CDD	Cumulative Dry Days	Days
CWD	Cumulative Wet Days	Days
EPD	Extreme Precipitation Days	Days
TP	Total Precipitation	mm/year
MDP	Maximum Daily Precipitation	mm/day

2.2.3 Historical Precipitation Performance Metrics

Dry, moist, and extreme precipitation anomalies are associated with distinct meteorological drivers. To evaluate the performance of CMIP6 model datasets, we evaluate how well they perform in aggregate in capturing all precipitation anomalies using the inter-annual variability skill score (IVSS) (Eq^n 1, Srivastave et al,2020).

$$IVSS_{m,i} = \frac{1}{N} \sum_{n=1}^{N} \left| \frac{IQR_{m,n,i}}{IQR_{o,n,i}} - \frac{IQR_{o,n,i}}{IQR_{m,n,i}} \right| \quad \text{....................................(1)}$$

Here, IQR is the interquartile range for an index i at location n, between a modeled dataset m and observed dataset o, where N is the total number of grid points in the dataset. A perfectly simulated model will have a IVSS value of zero, the larger the IVSS the poorer the performance of the model. To compare the relative performance of the model relative to other CMIP6 models, calculate the normalized interannual variability score (NIVSS, Eq^n 2).

$$NIVSS_{m,i} = \frac{IVSS_{m,i} - IVSS_{cmip6,median}}{IVSS_{cmip6,median}} \quad \text{......................................(2)}$$

Here, (IVSScmip6,med) is the median IVSS of index i across all CMIP6 models. A negative NIVSS value indicates that the model is performing better than most of the other models and a positive value indicates decreasing skill . This metric of comparing models based on NIVSS is known as evaluating the Model Variability Index (MVI). MVI is the median across all indices of a models NIVSS values. Models with a MVI value less than zero are considered the best performing models.(Chen, Jiang, and Li 2011; Jiang et al. 2015;Srivastave et al,2020)

For calculating performance metrics (NIVSS and MVI, Eq 1 and 2), precipitation indices were calculated for each grid at original model resolution. For comparison, the observed precipitation dataset (CPC) was resampled by nearest neighbor method to each model resolution (Table 2).

2.3 Interpreting future projections in the Great Lakes region:

2.3.1 Future scenarios:

CMIP6 has a set of eight different emission scenarios representing different potential futures called Shared Socio-economic Pathways (SSP). We evaluate precipitation changes in the Great Lakes region under two SSPs, SSP3-7.0 and SSP5-8.5. SSP3-7.0 is based on a world where countries focus on achieving energy and food security goals at any cost without collaboration. Policies are predicted to shift toward national and regional issues in this scenario. The radiative forcing in the SSP3-7.0 scenario reaches a level of 7.0 Wm-2 at the end of the 21st century. SSP5-8.5 is known as the “worst case” scenario as it is based on a world where economic development remains entirely dependent on fossil fuels. The radiative forcing reaches a level of 8.5 Wm-2 at the end of the 21st century in this scenario (O’Neill et al. 2016). These two scenarios, which are the highest emission scenarios in CMIP6, are used to allow for evaluation of significant response signals in the hydrologic cycle. A Mann-Kendall trend test is used to quantify projected changes in future (2015-2100) dry, moist, and extreme precipitation indices for the five models selected based on historical MVI for both extreme emissions scenarios.

2.3.2 Trend Estimation in Future Precipitation Indices

Five models based on their MVI values are selected to study further for future precipitation characteristics. To track the changes in future precipitation indices, a Mann-Kendall trend test was performed. It is a non-parametric test that is used to statistically detect a monotonic trend in a variable over time. The non-parametric nature of this test, it doesn't make any assumption about the normal distribution of the data. The null hypothesis here is there is no monotonic trend present and alternative hypothesis a monotonic trend is present. A significance level of 0.05 was utilized for this test. During the calculations of trendlines, the average value of an individual model's historical index was used as the y-intercept. Additionally, the slope was determined by regressing the anomalies from their mean historic value with the number of years. This was used to infer magnitude of projected 21st century changes in precipitation indices.

2.4 Circulation pattern analysis

2.4.1 CCA analysis:

After choosing models based on their MVI, their circulation anomalies were analyzed. We perform a canonical correlation analysis (CCA) between 500hPa geopotential heights anomalies in summer months and annual summer precipitation anomalies. CCA is a method to find association between two variables by reducing their features and maximizing the linear correlation among those two variables. As a first step of this analysis, we perform principal component analysis on geopotential height data, this helps to eliminate the non-significant features i.e., removes noise from the data. The number of principal components were selected in a way that explains at least 70% variance in the data. To reduce the noise in precipitation data we take the average anomalies in each lake basin's area.

Section 3: Results

3.1 Yearly Total Precipitation

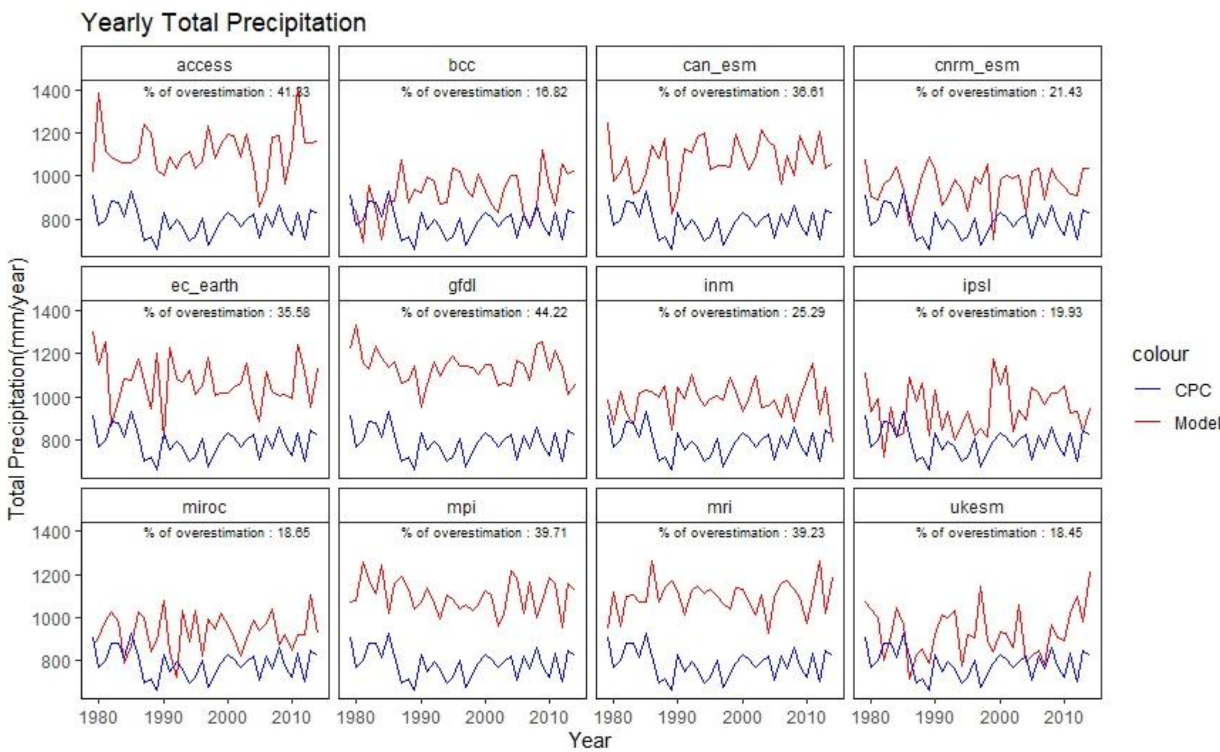

Figure 02: Yearly Total Precipitation in 12 CMIP6 Models over 1979-2014

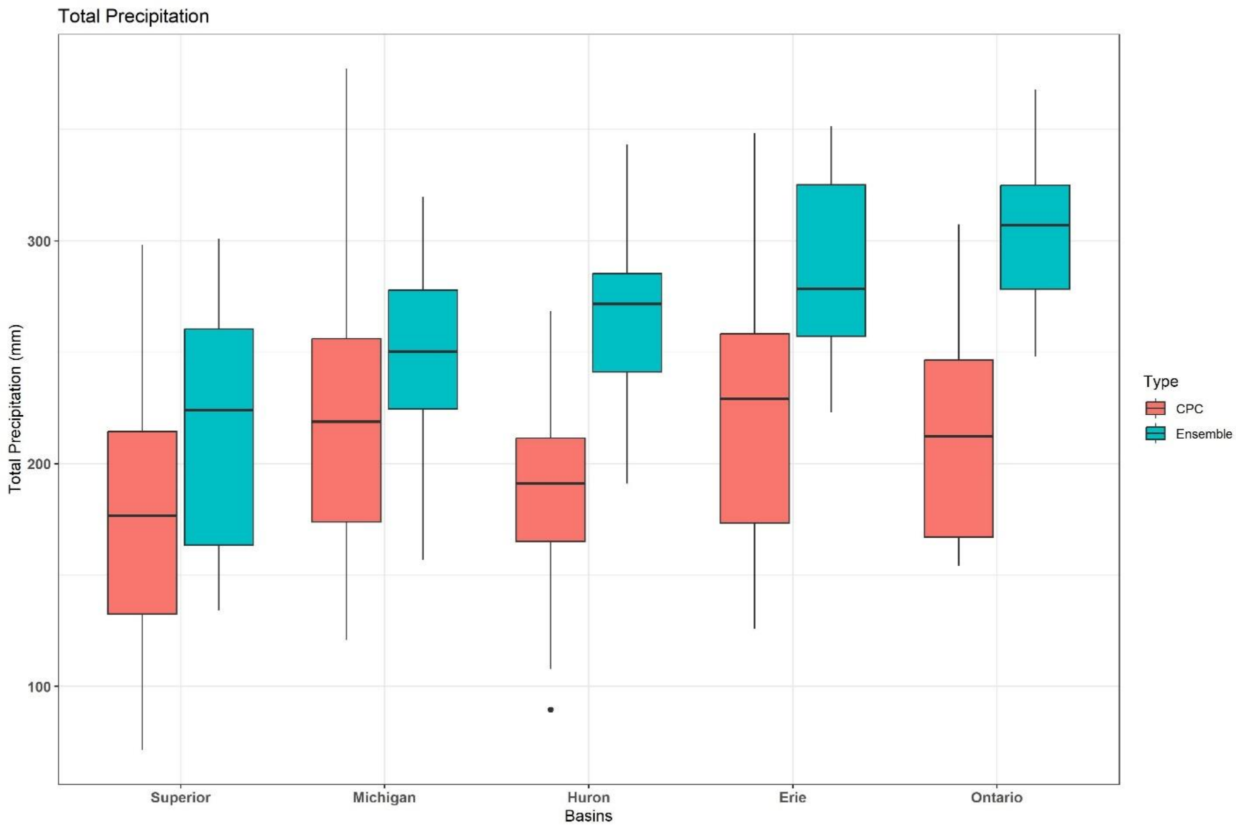

Figure 2a. Summer Total Precipitation by Basin in Ensemble Mean and Observed Dataset

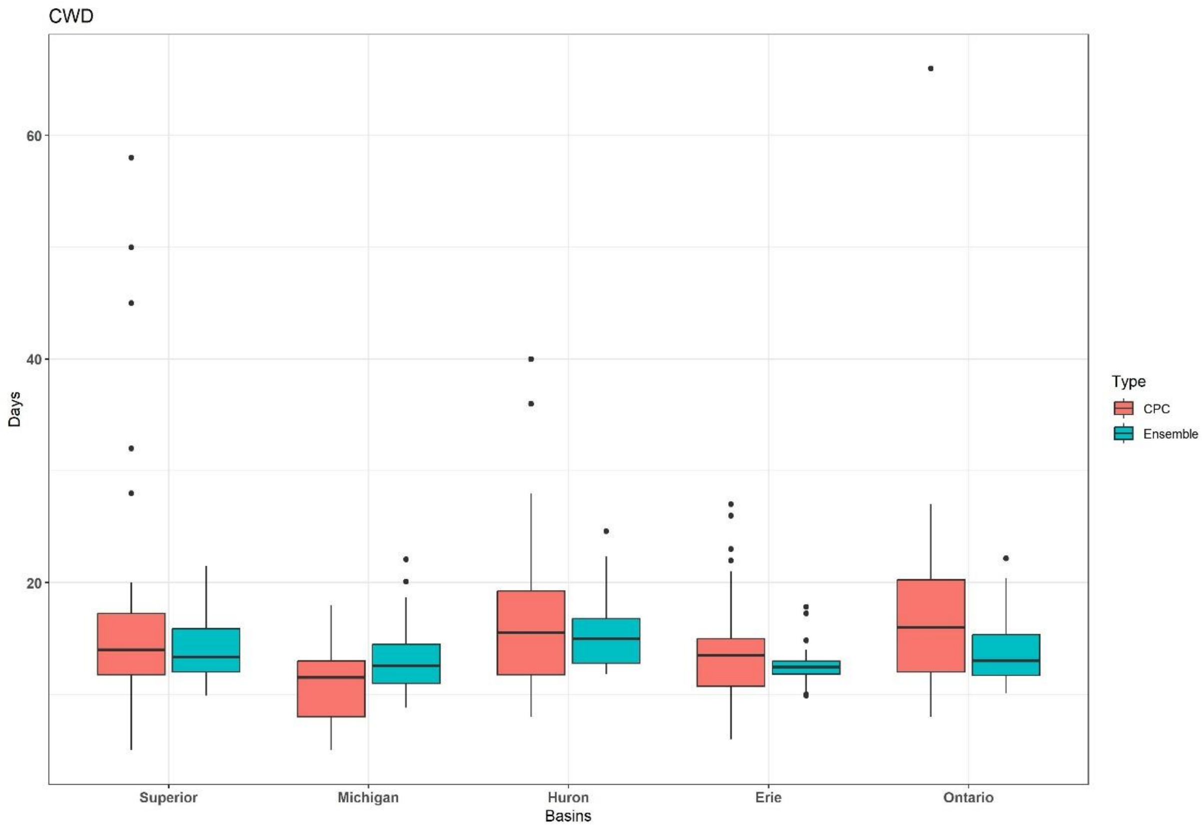

Figure 2b. Cumulative Wet Days by Basin in Ensemble Mean and Observed Dataset

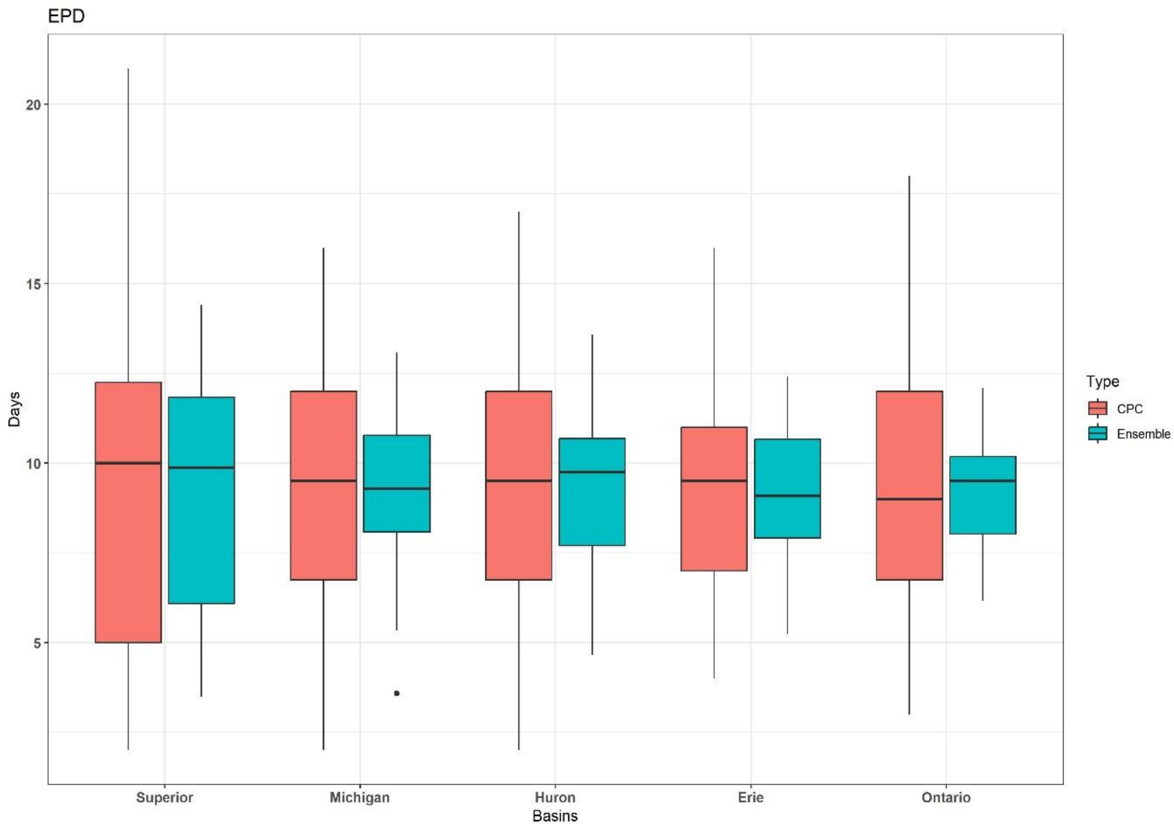

Figure 2c. Extreme Precipitation Days by Basin in Ensemble mean and Observed Dataset

Almost all candidate models show a consistent positive bias in annual total precipitation estimates. GFDL shows the strongest bias, with 44.22% overestimation of annual precipitation, followed by the models that show lower percentage of overestimation are BCC (16.82 %), CNRM_ESM (21.43%), IPSL (19.93 %), MIROC (18.6 %), and UKESM (18.45 %). When looking at the distribution of summer precipitation estimates by basin (Fig 2a), we see that the positive bias in total precipitation grows stronger as we move from west to east across the basin. While total precipitation is largely overestimated by the models (Fig 2a), both extreme precipitation days and cumulative wet days show comparatively little bias (Fig 2b,Fig 2c), suggesting that on average, CMIP6 candidate models are better able to capture climatological accuracy in precipitation duration. Strong positive overestimation in maximum daily precipitation, with a negative variance bias and strong intermodal agreement, is seen in the estimation of maximum daily precipitation (Fig S12), suggesting that origin of consistent overestimation in total precipitation in this region is not associated with inaccuracy in parameterizations related to frequency and duration of precipitation events, but in rainfall intensity. To explain how the biases exist on a seasonal scale, we look at the monthly average precipitation in the model simulations.

3.2 Monthly Average Precipitation

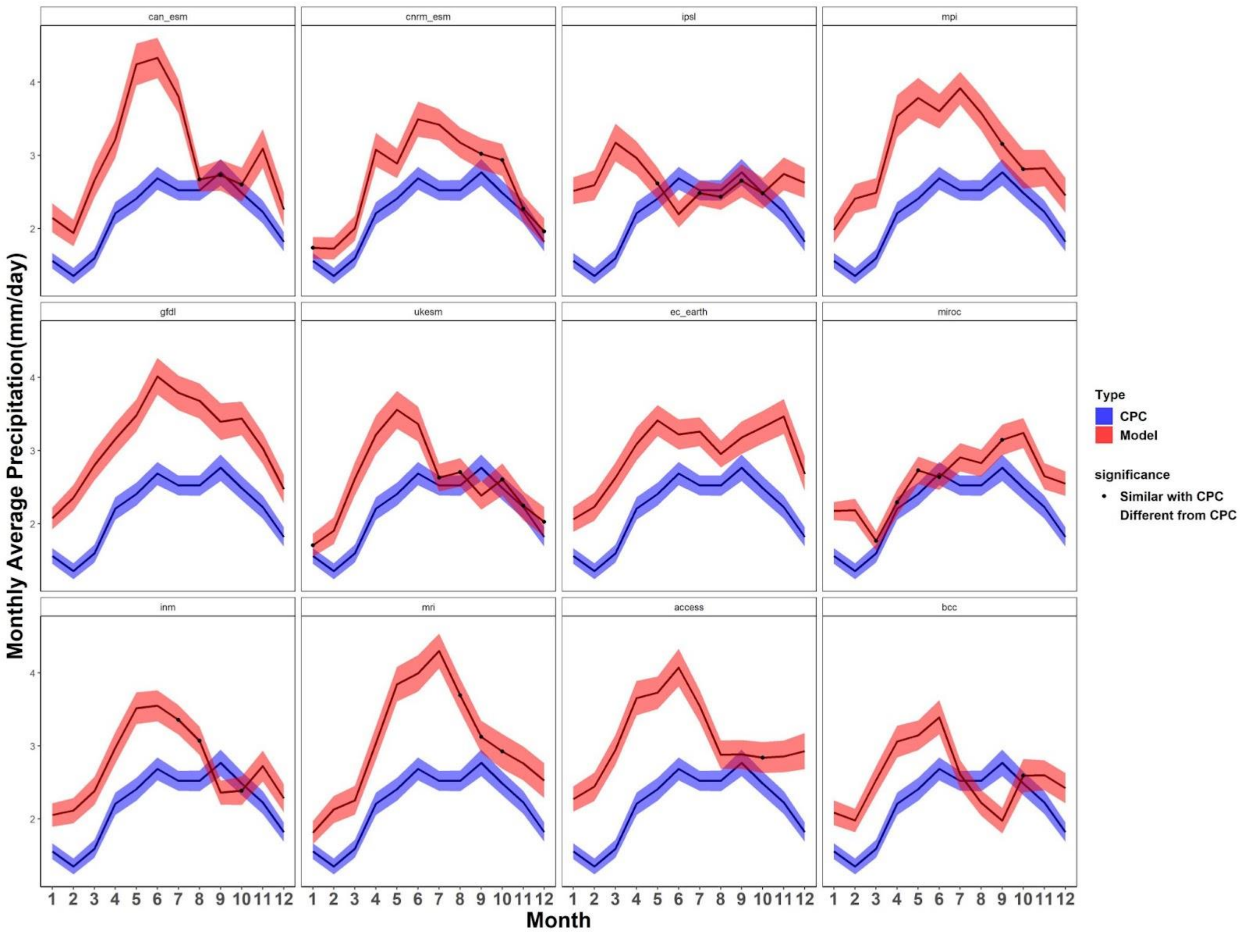

Fig 03: Monthly Average Precipitation in 12 CMIP6 Models and CPC Dataset

Nonparametric hypothesis testing is used to evaluate climatological bias in monthly precipitation estimates. Little agreement is seen between modeled monthly precipitation and observed monthly precipitation. Models that show some agreement tend to do so in fall or early winter months (MRI, ACCESS, MIROC, UKESM, INM, MPI, BCC, CAN_ESM, CNRM_ESM). The only model to show significant similarity in summer precipitation was MIROC Consistent with annual precipitation, positive or wet bias is observed in most models, particularly in the spring months. In addition to mean bias in monthly precipitation, models show greater interannual variability in monthly precipitation than CPC data, suggesting an overestimation of monthly precipitation variance.

3.3 Model selection

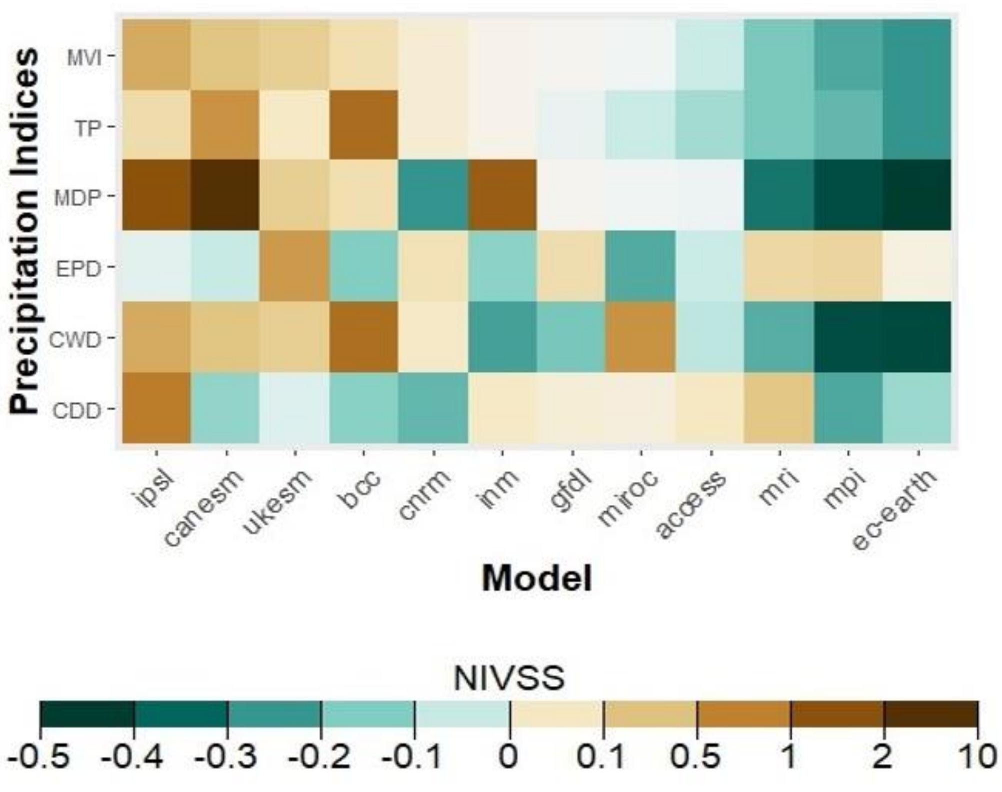

Fig 04: A Portrait Diagram of Normalized IVSS over the 1979-2014 Period.

Figure 04 shows the NIVSS for all precipitation indices in the CMIP6 models. A model MVI is shown in the top row, which is the median of IVSSs over all indices for that model**.** For a given index, the NIVSS is calculated by normalizing the respective IVSS with respect to the median IVSS over all the CMIP6 models. The median IVSS serves as a threshold value for each index. The topmost row is the MVI value, the median of NIVSS all the indices for an individual model. It serves as an integrative metric of model performance. A model with a negative MVI value is considered to have higher accuracy relative to other models. We get 5 models with a negative value, which were chosen for further analysis. They are Ec-earth, MPI, MRI, MIROC and ACCESS. These 5 models were used to examine the trends in future precipitation indices.

In general, the higher performing models overall consistently showed good agreement in inter-annual measurements of moist anomalies (total precipitation, maximum daily precipitation, and cumulative wet days). These models did not necessarily do as well in predicting dry anomalies (cumulative dry days). Several models that performed well overall, such as Ec-earth and MPI, showed reasonable agreement with cumulative dry days. Similarly, several models with less accuracy in predicting moist anomalies (CNRM and Can-ESM) were more effective in predicting cumulative dry days.

3.4 Cumulative Dry Days

Models with negative MVI values have similar variability as the observed cumulative dry days (Fig S1). ACCESS is the one model that has similar means as observed in all lake basins. In Lake Superior most numbers of models show similar means and least number of models in Lake Huron. IPSL overestimates the median precipitation distribution in all the lake basins, but the degree of overestimation is higher in Lake Erie and Lake Ontario. INM on the other hand underestimates the distribution most also in Lake Erie and Lake Ontario, which indicates that both positive or negative bias could be more prominent in eastern great lake basins (Fig S2). The spread of the distribution in general is higher for models than observed cumulative dry days which is opposite of what was found while looking at the ensemble mean of all models (Fig S3).

3.5 Cumulative Wet Days

Lake Huron has the lowest variability in observed cumulative wet days, even models with negative MVI values do not capture it well (Fig S4). For Lake Erie the median value of cumulative wet days in the models are either close to the observed value or lower than that. The range of the distributions are mostly lower (except in INM) than observed distributions. Lake Huron has a mix of models overestimating (MPI, MRI, INM, CAN_ESM) and underestimating (UKESM,MIROC, INM) the median wet days. IPSL and BCC are the two models here that have similar mean cumulative wet days as observed. In Lake Michigan, only MRI has a similar mean value as observed. Most models present a lower than observed median value in this basin area, so is true for the variability. In Lake Ontario, INM is the only model that has a similar mean wet day, all models are similar or lower than observed value. For Lake Superior, GFDL and BCC have similar mean wet days as observed. Median cumulative dry day values are underestimated in all the models except in INM. The variability in wet days has a mix of positive and negative bias in this basin. It appears upper western lake basins i.e., Lake Huron and Lake Superior have both high and lows of wet day variabilities, which makes it cancel out these biases while calculating ensemble means and capture the variability closer to the observed one (Figure S6).

3.6 Extreme Precipitation Days

Almost all models show similar variabilities in Lake Superior as observed, except IPSL, which underestimates the variability (Fig S7). A comparable situation is also noticed for Lake Michigan. For Lake Huron models with negative (positive) MVI values tend to have lower (higher) than observed variability. Variabilities in Lake Erie and Lake Ontario do not appear to have any consistency with their MVI values. While comparing the mean values we see in all basins they show a similar mean with the observed data (Fig S8). These similarities may change upon the definition used for extreme precipitation. While comparing ensemble mean extreme precipitation days an underestimation in variability emerges which gets worse west to eastwards(Fig S9).

3.7 Maximum Daily Precipitation

In all lake basins, models overestimate both the median maximum precipitation intensity and the variability (Fig S10). This degree of overestimation is higher for eastern Great Lakes basins i.e., Lake Erie and Lake Ontario. Models with higher MVI values in Lake Erie and Lake Ontario tend to also overestimate variance in these two basins (Fig S11). The highest number of models with comparable means are found in Lake Erie and Ontario, the least is seen in Lake Michigan and Lake Superior. These features make the ensemble mean distribution overestimate the maximum precipitation in all basins (Fig S12)

Total Precipitation

For Lakes Superior, Huron and Michigan, MIROC is the only model with a negative MVI value that underestimates the amount of total precipitation (Fig S13). The variability and median are also underestimated in this model. In Lake Erie, UKESM and BCC have similar average total precipitation. The majority of the models overestimate both the median total precipitation and the variability (except UKESM,BCC,IPSL). In Lake Huron, the variability has a positive bias in all models, and no model has produces an accurate mean. In Lake Michigan, models have the most inconsistencies in their distribution. Though the variabilities in the models have consistent positive bias, the median values do not. Models behave in a similar way in Lake Ontario as in Lake Erie, the median estimations are the same for the models in both basins. Overall, a higher median is found in the ensemble mean and the variability diminishes as we go to eastward basins. (Figure S15).

3. 6 Future Precipitation

Cumulative Dry Days

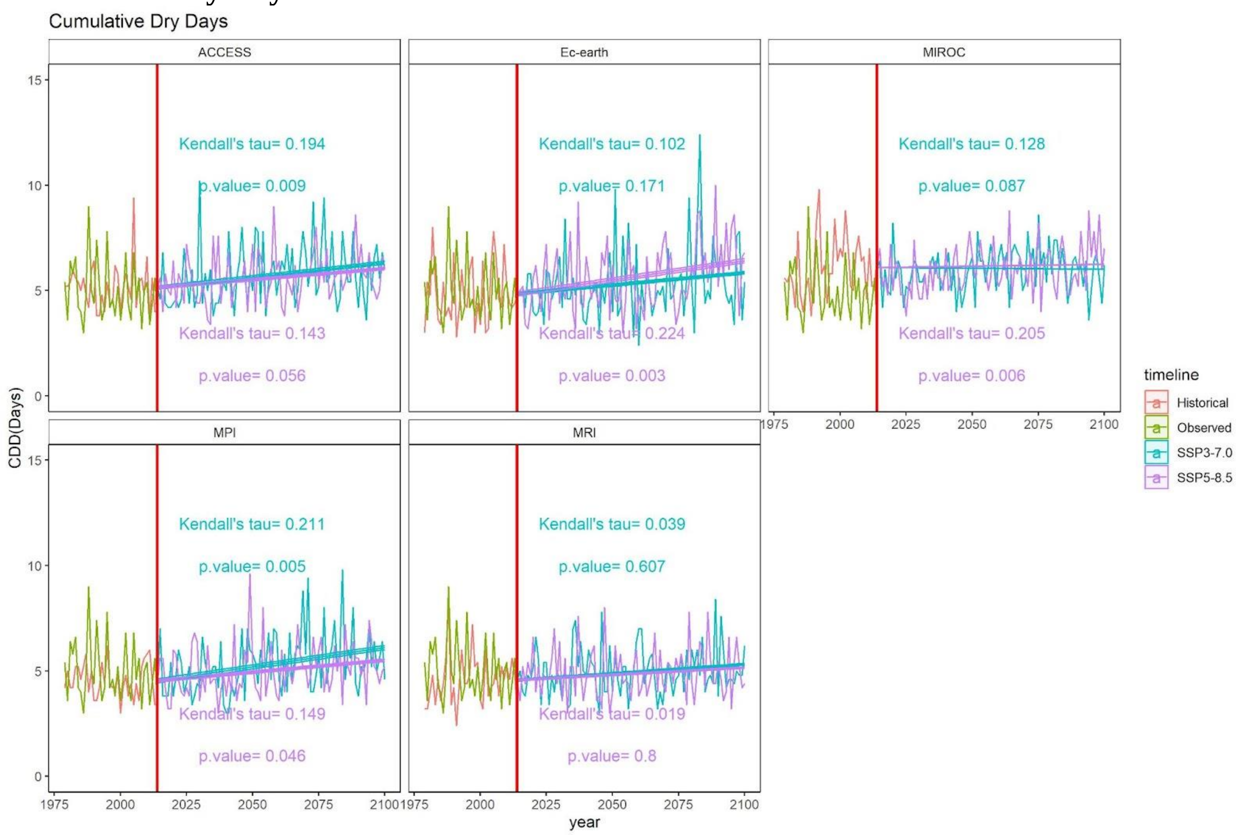

Figure 05: Trends in Cumulative Dry Days

Figure 05 shows projected trends in cumulative dry days (CDD) in two different emission scenarios. All five models exhibit an increasing trend in cumulative dry days in all scenarios. MPI and EC-earth, which among these five models showed the greatest fidelity in capturing historical interannual variability in CDD, both suggest a statistically significant increase in CDD under both warming scenarios, with 0.211 (0.149 in SSP5-8.5) and 0.102 (0.224 in SSP5-8.5) additional dry days expected per year by the end of the century. While ACCESS showed little skill in capturing historical interannual variability in CDD, it projects increases in CDD that mirror MPI and EC-earth. Oddly enough, in the MPI model, greater increases in CDD are projected for the SSP3.7 scenario than the SSP8.5 scenario. No significant future trends in CDD are observed in MIROC and MRI models. Like ACCESS, neither MIROC nor MRI showed skill in capturing historic interannual variability in CDD (Fig S3).

Cumulative Wet Days

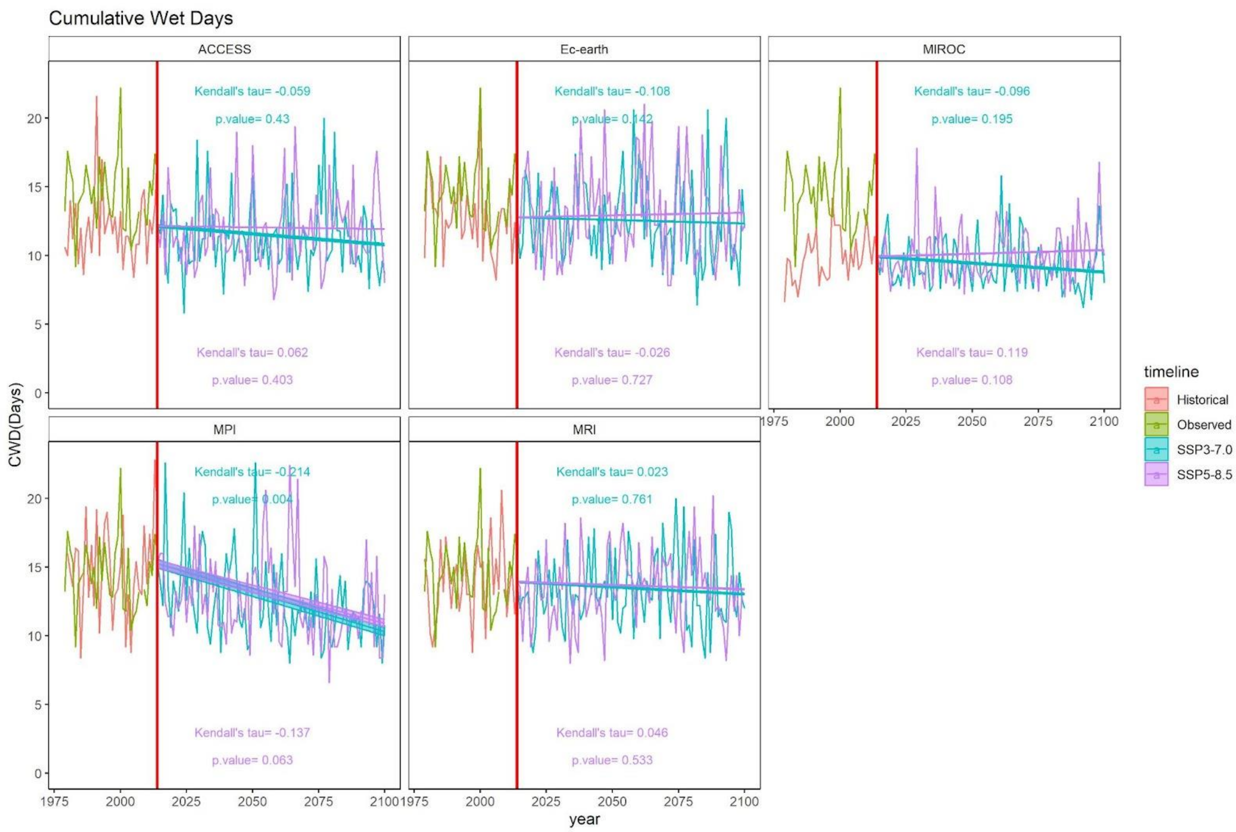

Figure 06: Trends in Cumulative Wet Days

Figure 06 shows projected trends in cumulative wet days in two different emission scenarios. In historical simulations, MRI, MPI, and EC-Earth showed the greatest still in capturing interannual variability in CWD, yet there is little consensus between these models on future trends in cumulative wet days. MPI predicts strong negative trends in CWD, with a decrease in wet day sequence of about 0.214 (0.197 in SSP5-8.5) days predicted by the end of the century. The remaining models predict a slightly negative to neutral trend. In the SSP3-7.0 scenario, except MRI all other models have a decreasing trend in the future. Among these decreasing trends only MPI has a significant one. For the SSP5-8.5 scenario, mpi shows a decreasing trend. MRI showing an increasing trend compliments their comparably weaker than others positive trend found in the cumulative dry days.

Extreme Precipitation Days

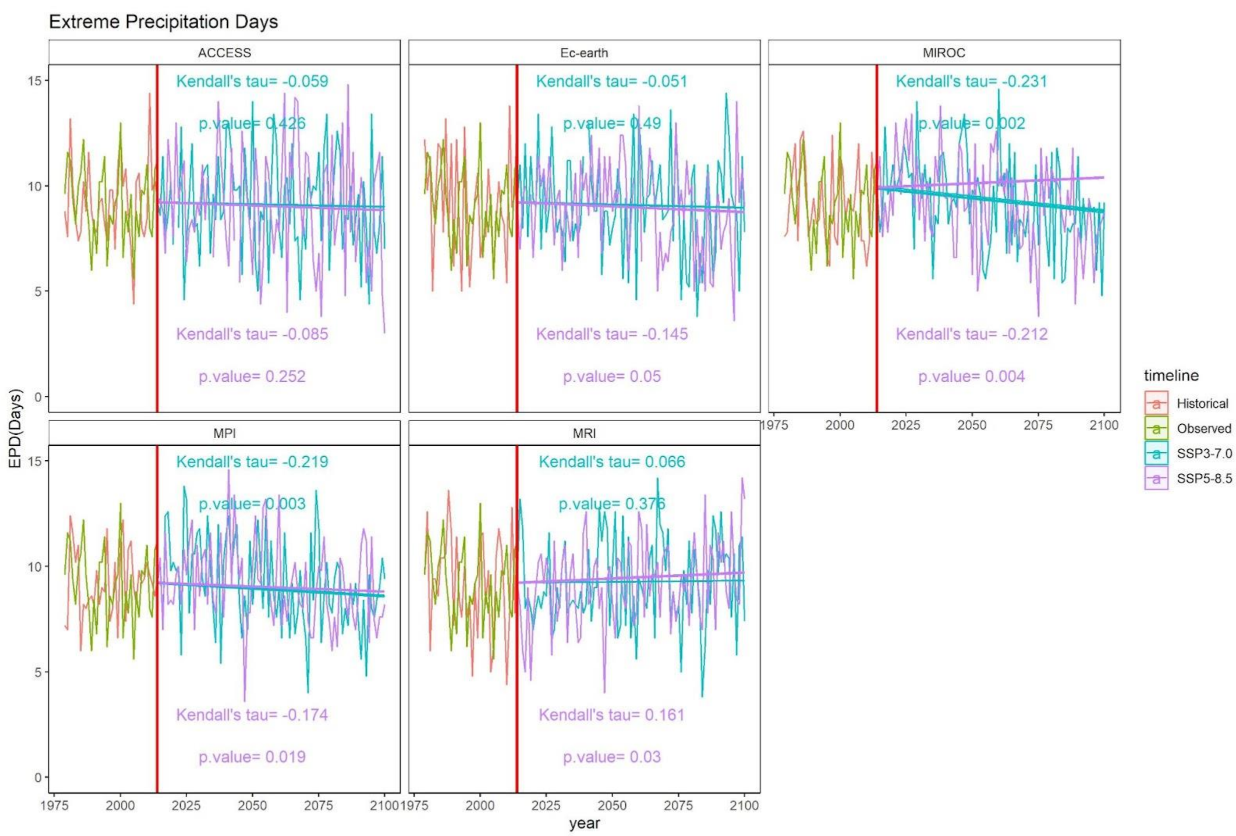

Figure 07: Trends in Extreme Precipitation Days

Figure 07 shows projected trends in extreme precipitation days in two different emission scenarios. ‘MIROC’ and ‘MPI’ show a significant decreasing trend in both scenarios. Ec-earth has a significant decreasing trend in SSP5-8 but not in SSP3-7.0. ‘MRI’ is the only model that exhibits increasing trends ,though only the trend in SSP5-8.5 appears to be significant. It complements the case of 'MRI' projecting increasing trend in wet days. Trends tend to be more apparent in higher emission scenarios, even after their disagreements about the sign of change.

Maximum Daily Precipitation

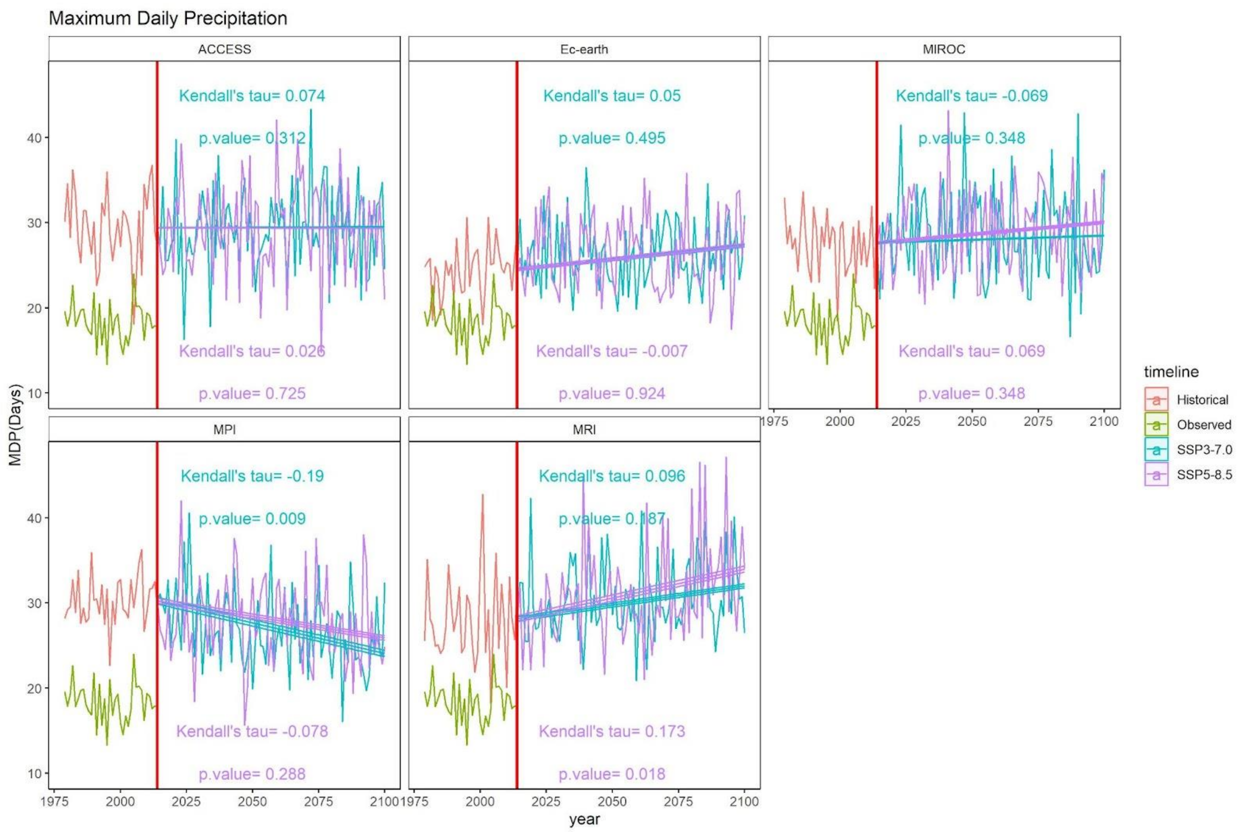

Figure 08: Trends in Maximum Daily Precipitation

Figure 08 shows projected trends in extreme precipitation days in two different emission scenarios. MPI is the only model that exhibits a decrease in maximum daily precipitation in both emission scenarios; the decreasing trend only appears significant in the SSP3-7.0 scenario. MIROC shows a weaker decreasing trend in the SSP3-7.0 scenario but not in SSP5-8.5. The reverse is observed in the case of Ec-earth. None of these trends emerge statistically significant. MRI exhibits an increasing trend in both the scenarios but only the trend in SSP5-8.5 is significant.

The discrepancies in the sign of changes in maximum precipitation intensity in different emission scenarios supports the idea that extreme precipitation intensity may not be dependent on emission scenarios (Pendergrass et al. 2015).

Total Precipitation

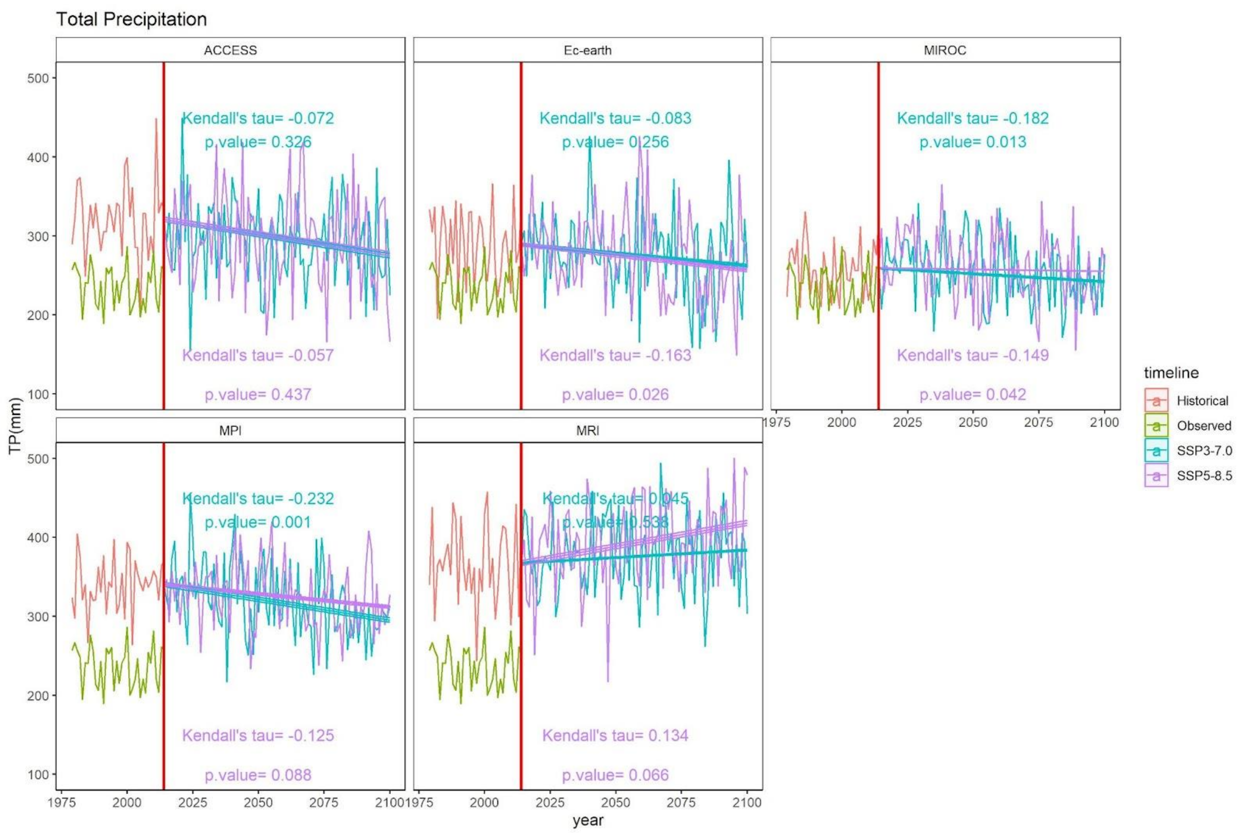

Figure 09: Trends in Total Precipitation over 2015-2100

Figure 09 shows projected trends in total precipitation days in two different emission scenarios. Most models except MRI predict a decrease in total warm season precipitation. For MIROC the decrease is significant in both emission scenarios. 'Ec-earth' exhibits a significant decrease in SSP5-8.5 but not in SSP3-7.0 ,while the opposite is found for MPI. MRI predicts an increase like it did in other wet index functions, but they do not appear statistically significant.

Most models showing a decrease in total precipitation lies in line with the projection of a drier summer in the midwestern US (Dollan et al. 2022)

Circulation Anomalies

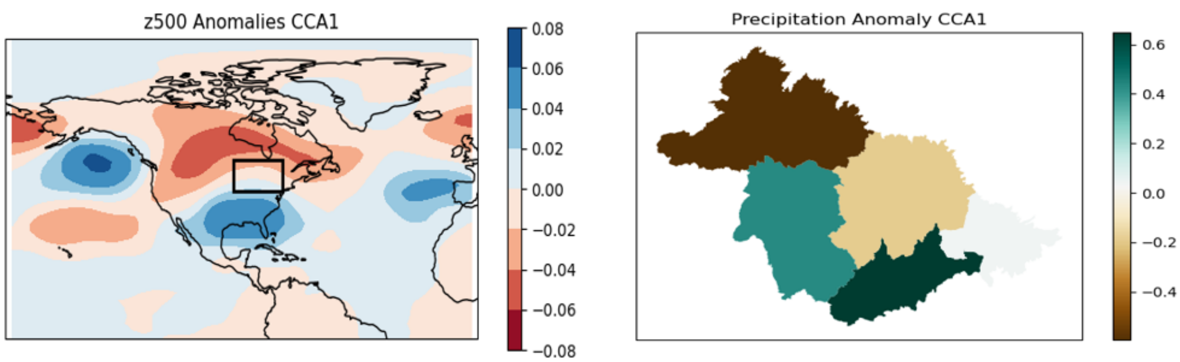

Figure 10: Circulation anomalies for z500 geo-potential height and averaged summer precipitation

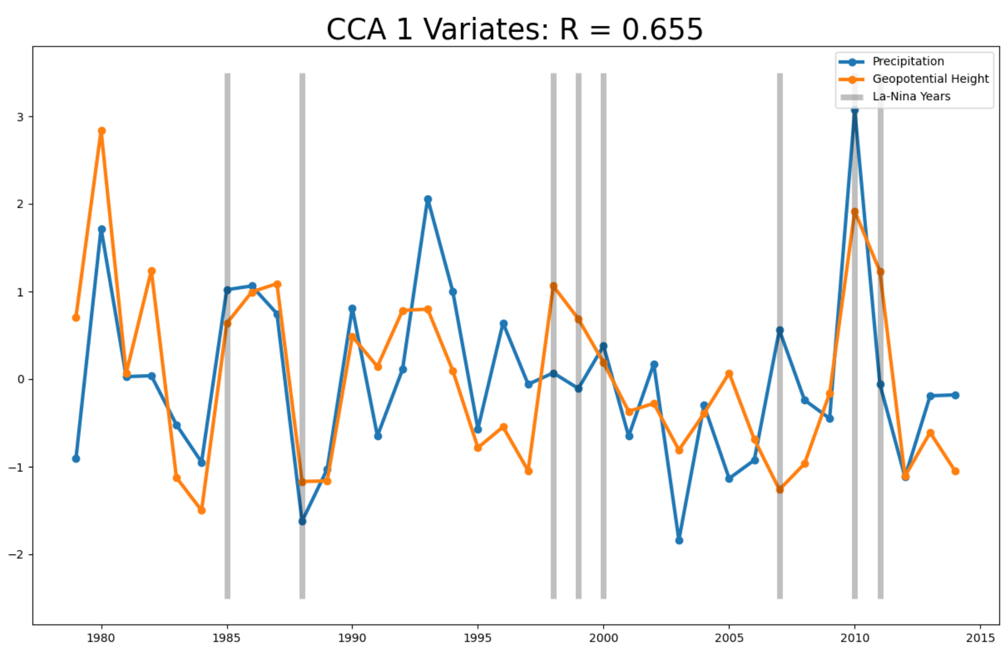

Figure 11: Normalized time components of CCA1 for observed dataset.

Figure 11 shows the pattern of the dominant geopotential height and precipitation anomalies from CCA of historical meteorological observations (CPC Precipitation and NCAR/NCEP reanalysis). The first variant CCA shows a strong ridge above the Great Lakes region. A high-pressure center in the western pacific is observed, which normally is seen in a La-Nina pattern. Summertime La-Nina cycles were observed in 1985, 1988, 1998, 1999, 2000, 2007, 2010 and 2011(NOAA's Climate Prediction Center 2001) From the time series plot of 1st variant of CCA between precipitation anomalies and geopotential height anomalies we see these are the years (except 1988 & 2007) where both variables show positive anomalies. The wet anomalies in the southern Great Lakes can be explained by this pattern. The precipitation anomalies may not appear much prominent because of La-Nina patterns mostly being strong in the winter season. Another high-pressure center can be seen in the Gulf of Mexico region. Lake Erie is the main driver of precipitation anomaly in this pattern.

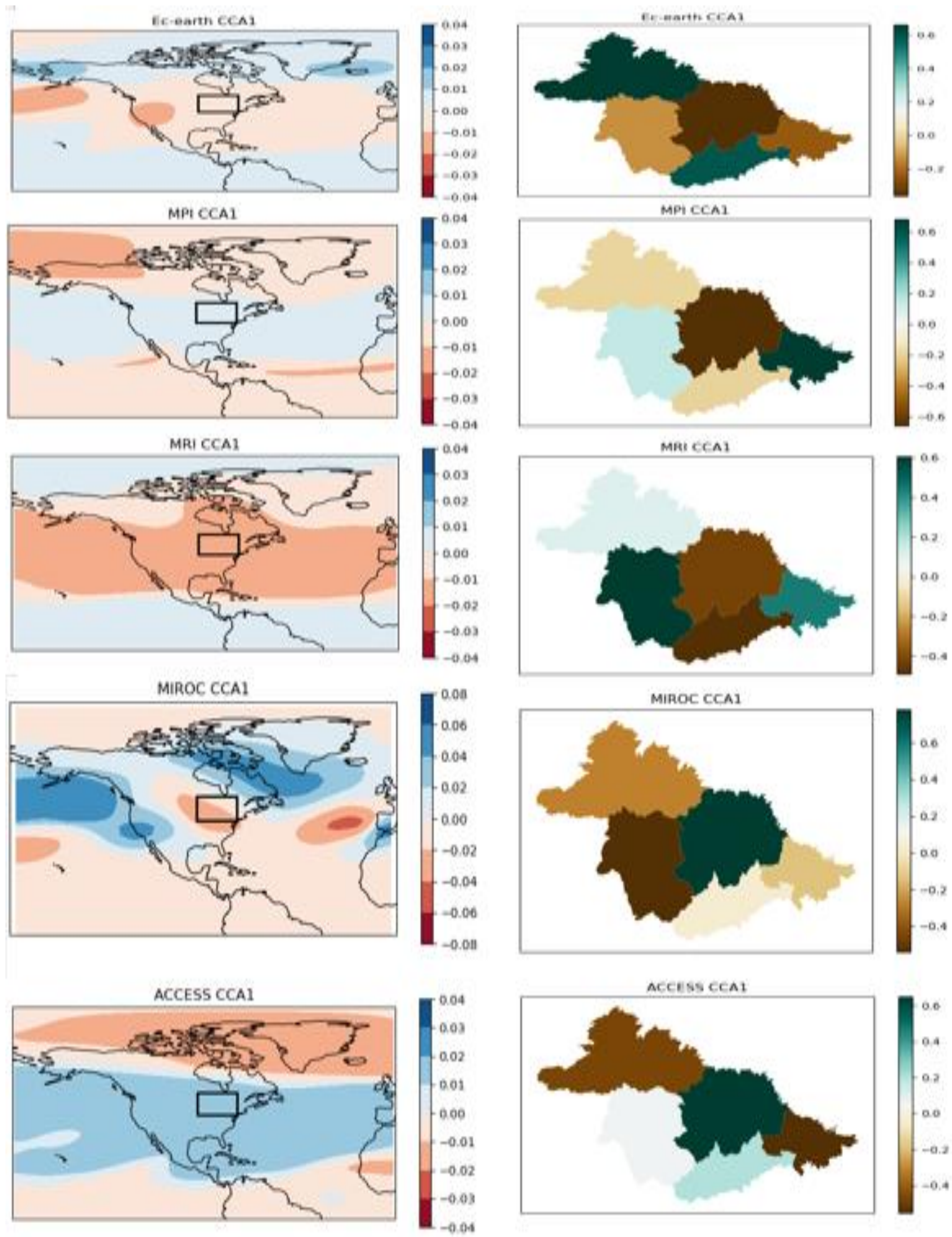

Figure 12: Circulation anomalies for z500 geo-potential height field and averaged summer precipitation anomalies in each lake basin for 5 selected models based on their MVI.

For most models, the geopotential height anomaly pattern in this isn't as coherent as seen in the observed first variant of height anomalies. The ridges and troughs aren't clearly understandable from the height patterns and there is very little spatial variation. MIROC appears to be the only model that shows some spatial variation in their height anomalies; it has a positive anomaly centered in the western pacific as seen in the dominant observed pattern, but it spans through a larger area than what we found in the observed pattern. It also doesn't show any significant wet anomalies in the La-Nina years (not shown). The strong ridge seen in the observed pattern in the great lakes transboundary is missing in all the model simulations. In terms of the dominant precipitation pattern, in the observation wet anomalous condition is found in Lake Michigan and Lake Erie and dry anomalous condition is found in Lake Ontario, Lake Superior and Lake Huron. MIROC, ACCESS and MPI also have the similar dry anomaly in Lake Superior, but it's not seen in Lake Erie in these models. The wet anomalies do not have any consistency among the models.

Section 4: Discussion

General circulation models participating in coupled model intercomparison project experiments have shown notoriously low fidelity in capturing hydrometeorological and hydroclimatic variability in the Midwestern and Northeastern United States (Akinsanola,2020 ; Minallah and Steiner, 2021b), particularly during summer months (Peltier et al,2018). This limits effective planning for water resources management in the Great Lakes basin, which contains over 25% of global freshwater resources. This is particularly true for the management of hydroclimatic extremes, such as droughts and floods. This analysis aims to investigate how a wide range of models participating in the latest CMIP experiment, CMIP6 perform in capturing several different indices of extreme dry, moist, and wet precipitation.

Uncertainties in CMIP6 model predictions are associated with both internal variability and model uncertainty. These model uncertainties, which can be observed as biases in historical simulations, will likely be conveyed in future projections (Amal et al, 2022). Almost all candidate models show a consistent positive bias (17-44% depending on the model) in annual total precipitation estimates relative to CPC precipitation. The positive bias in total precipitation grows stronger as we move from west to east across the basin, which is an important meteorological signal for regional planning and management. If we do in fact end up with a climatological increase in precipitation that is stronger on the eastern range of the Great Lakes basin, this could be associated with increased flood risk on the eastern edge of the basin, which integrates anomalous flow across all the upper Great Lakes. While total precipitation is largely overestimated by the models (Fig S15), both extreme precipitation days and cumulative wet days show comparatively little bias (Fig S9 and Fig S6), suggesting that on average, CMIP6 candidate models are better able to capture climatological accuracy in precipitation duration. Strong positive overestimation in maximum daily precipitation, with a negative variance bias and strong intermodal agreement, is seen in the estimation of maximum daily precipitation (Fig S9), suggesting that origin of consistent overestimation in total precipitation in this region is not associated with inaccuracy in parameterizations related to frequency and duration of precipitation events, but in rainfall intensity. Individual GCM's bias towards overestimation of precipitation amount in a yearly scale were found in previous literature (Li et al,2014; Lun et al,2021). We found the results of our analysis clearly echo modeling uncertainties noted by other researchers analyzing CMIP ensemble precipitation predictions in North America.

Consistent model biases in climatological precipitation show seasonal patterns as well, with weak agreement observed between modeled and actual precipitation in fall/winter months for some models (MRI,ACCESS ,MIROC,UKESM,INM,MPI,BCC, Can-ESM, CNRM_ESM), and little (MRI) to no skill seen in predicting climatological warm season precipitation. The relative accuracy of cold season model predictions has been observed in the literature, and is likely attributable to the fact that while winter precipitation anomalies largely occur in response to large scale circulation anomalies, particularly ENSO and the PNA, summertime circulation anomalies are associated with small scale convective process (Li et al,2010) and lesser-characterized, more volatile modes of anomalous large scale circulation, such as dynamics associated with the development and decay of the summertime peak of the North Atlantic Subtropical High (Li et al,2011, Zorzetto et al, 2021).

Historic precipitation shows the most inconsistencies in wet indices. Previous literature suggests that the overestimation of wet indices may stem from the "drizzle problem" in general circulation models, where too much low frequency, high intensity precipitation is simulated (Gibson et al. 2019, Dai and Trenberth, 2004). This claim is strongly supported by our analysis, which shows strong positive bias in maximum daily precipitation across the Great Lakes basin, and a low variance bias in cumulative wet days. As positive moisture anomalies can result from either short duration high intensity storms, or long duration low intensity storms, our patterns in Maximum Daily Precipitation and Cumulative Wet Days suggest that we are overestimating the relative contribution of the former to total precipitation delivery in the region. Models also struggle to capture the spatial precipitation variability among each lake basin, which is more prominent in the indices of precipitation intensity. Using the ensemble mean doesn't resolve these inconsistencies. In some indices (EPD) spatial bias is observed from western to eastern lake basins.

The 5th Assessment Report of Intergovernmental Panel on Climate Change (IPCC) uses two metrics to identify GCM model performance to global forcings. The Equilibrium Climate Sensitivity (ECS), which evaluates the models' long term rebound to climatological stasis after an instantaneous doubling of atmospheric CO2, and the Transient Climate Response (TCR) evaluates the models projected equilibrium response to an incremental increase in atmospheric CO_2 (Tokarska et al. 2020; Nijsse, Cox, and Williamson 2020). The five models identified as higher performing in the Great Lakes region all have ECS and TCR values identified in the range of "likely warming" by the IPCC, building confidence in our findings. Our work suggests that resolution of models may not have much effect on finding statistical similarities in precipitation characteristics as it was supposed.

Evaluating future hydroclimate from the perspective of these climate models indicate that we may expect to see a drier summer in the Great Lakes region, which is consistent with results from other studies in Midwestern and Northeastern US (Zhou, Ruby Leung, and Lu 2022; Richard Peltier et al. 2018; Akinsanola et al. 2020). Summertime drying, associated with both a decrease in total precipitation and an increase in cumulative dry days, could be associated with ea strong ridge over the central United States, which weakens the storm track in the midwestern region and causes blocking in the late summer season (Chen et al, 2022). Less precipitation may also be driven by a thermodynamic reduction in atmospheric moisture content in this region in the months of July and August (Minallah and Steiner 2021a). Drier summer causes a net decrease in the net basin supply (Mailhot et al. 2019). Among our five selected models only one (MRI) predict a decrease in the dry index (Cumulative Dry Days). This may be attributable to a very high value of $\Delta P/\Delta T$ (percentage of change in precipitation per degree kelvin) in the MRI model relative to other ensemble members (Pendergrass et al. 2015).

Shifts in the seasonal precipitation cycle in the Great Lakes are observed, with an earlier onset of spring, and an increase in the relative contribution of total annual precipitation during the winter months (Minallah and Steiner 2021b; Labe, Ault, and Zurita-Milla 2016). The reductions in cumulative wet days and total precipitation are associated with an increase in maximum one day precipitation Similar trends are also found in Akinsanola et al,(2020) and Dollan et al., (2022). This suggest there may be an increase in future likelihood of more severe extreme events, marked by precipitation intensity, clearly mirroring the “wet gets wetter”’ characterization of thermodynamic intensification of the hydrologic cycle under climate change (Li et al. 2021). This pattern was also found in CMIP5 higher emission scenarios (Shrestha et al. 2022). This increase in extreme rainfall events is expected to scale with the 7% increase per 0C warming and be originating from higher altitudes where moisture is more available(d’Orgeville et al, 2014).

The changes in growing season precipitation will have an impact on the agriculture management practice and ecology in this region. It will affect the transport of nutrients in the lakes. It can modify the magnitude and timing of nutrient loading and disrupt the balance of the lake ecosystem (May et al, 2022). Crop yields for some kind of dominant crops in this region may drop, which requires an alternative agricultural plan to adapt with these changes (Liu and Basso 2020). More frequent extreme events will result in more run-off, which may affect the water quality in the lakes. This can also pose a threat to safe drinking water supply (D. Wang et al. 2022).

The primary mechanism of precipitation delivery in the summertime in the Great Lakes region is convective recycling, which is a fairly small-scale processes (Li et al, 2010). General circulation models are not able to capture these small-scale processes due to their coarse resolution. Evaluating models capability of replicating large scale circulation patterns depend on type of precipitation indices being used, it can the explain the extreme events more clearly than for average precipitation (Agel and Barlow 2020; Agel and Barlow 2017; Paxton et al. 2021). For seasonal precipitation the signals may be too smoothed out to find any distinct dominant pattern in them. The teleconnection patterns are also more evident in winter season in this area, so meteorologic influences on precipitation are more apparent in winter than summer. Future work will analyze how summer precipitation in the Great Lakes region can be explained mechanistically from general circulation models.

Section 5: Conclusion

The goal of this study was to identify which models demonstrate the most physical fidelity in capturing circulation anomalies related to seasonally and climatological variability in Great Lakes precipitation, so that appropriate models can be selected to promote insightful policy planning to mitigate the effects of a changing climate. Relative performance of models against observed precipitation was assessed using NOAA CPC unified gauge adjusted dataset. The quantification of model performance was done by the calculation of Model Variability Index (MVI) which is a comparison between IQR ratios. Models selected based on MVI values were used to estimate the trends in future precipitation in two different emission scenarios.

Based on the MVI, five models, 'Ec-earth', 'MRI', 'MPI', 'ACCESS', 'MIROC' demonstrated the least amount of error in capturing the historic variability in Great Lake Regions hydroclimate. According to these five models, model performance in mirroring historical observation depends on the category of index function, models who have better skill in capturing historic variability may still differ in their future projections. An overall drier future with longer dry spell is expected from the selected models.

Climate models are developed to capture complex interactions among different components of the earth system. Even though this work attempts to select models based on historical accuracy, these metrics may not be enough to cover the full scope of hydrometeorological accuracy of a climate model. Model performance metrics may be biased by the choice of observational dataset, choice of precipitation index function, choice of timeline, extent of region for analyzing the large-scale anomalies, the statistical methods used. Inclusion of more models, evaluation for other seasons and a more detailed spatial analysis would be necessary to make a conclusive decision about selecting climate models which are representative of the Great Lakes region. Despite limitations this study provides a guideline to make more meaningful predictions about future hydroclimate in the great lakes basins, which is expected to be useful for a more intricate analysis in future.

Section 6: APPENDIX

CDD

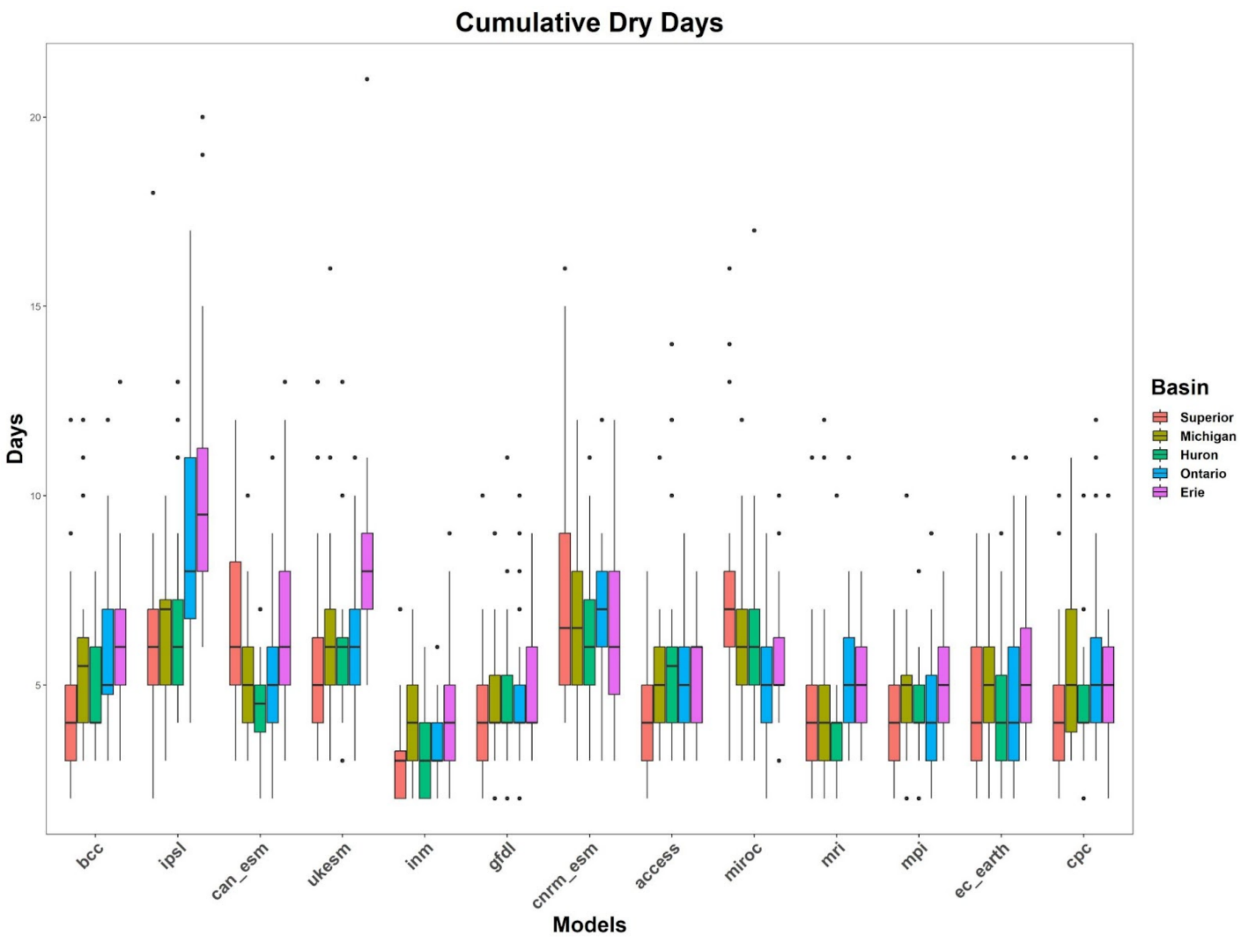

S1: Box and whisker plot for cumulative dry days aggregated over lake basins

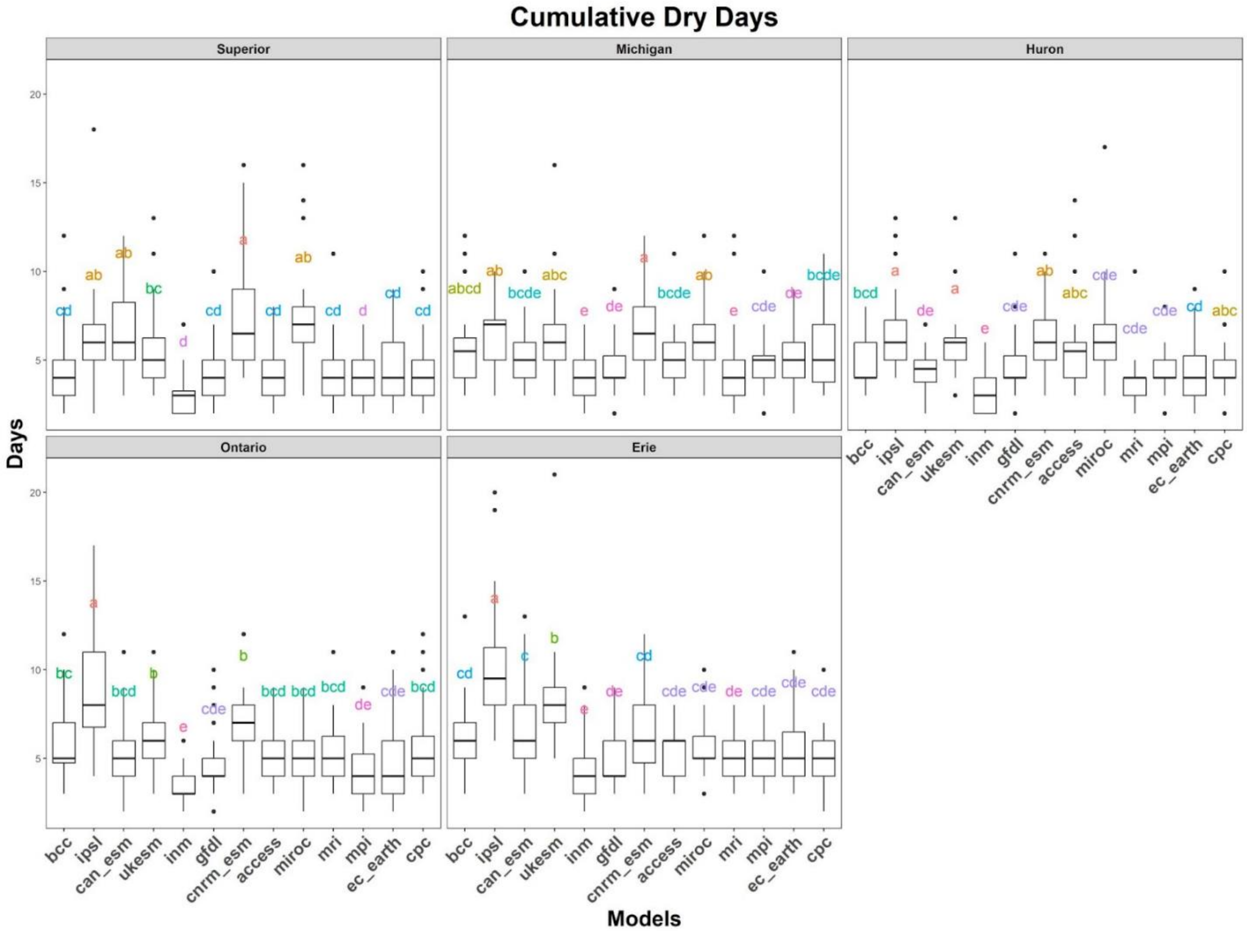

S2: Box and whisker plot for cumulative dry days aggregated over lake basins with letters to show the significance difference among the means in each lake basin

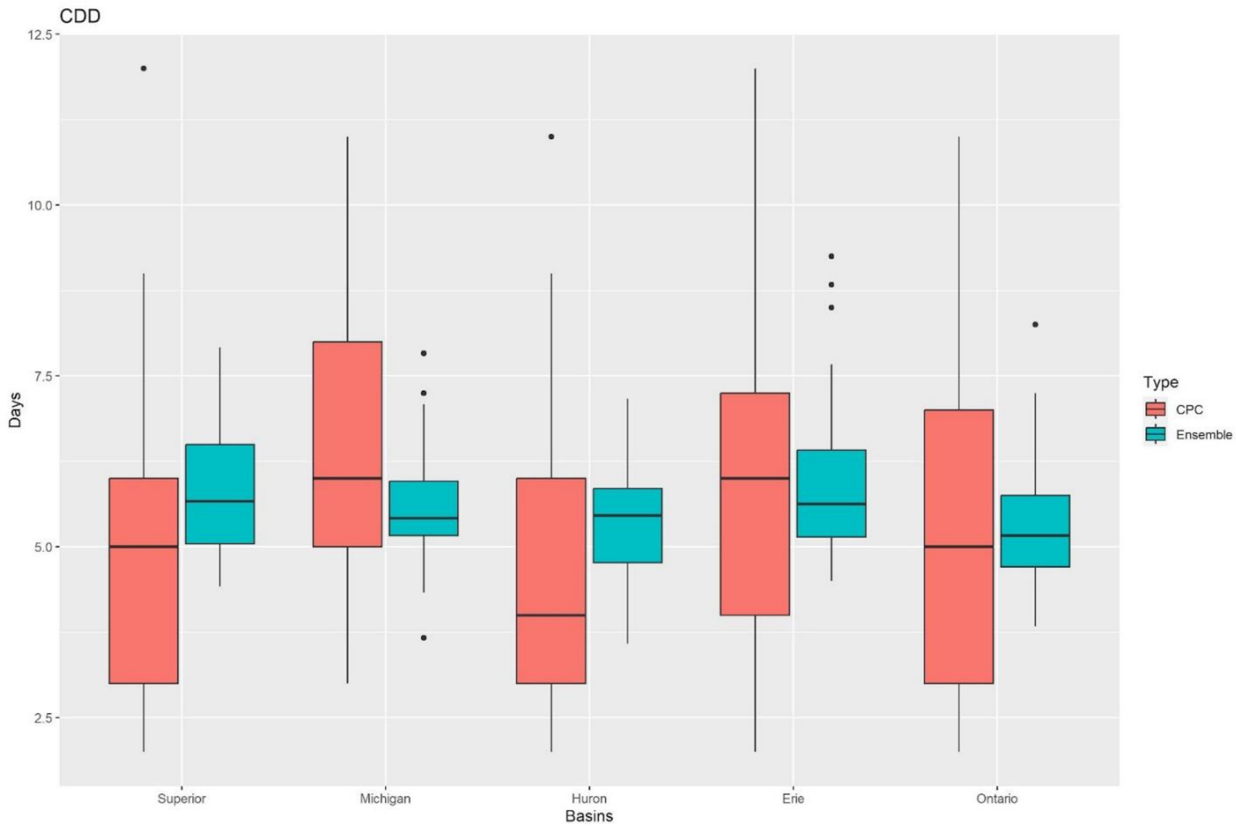

S3: Box and whisker plot for cumulative dry days aggregated over lake basins in ensemble mean and observed precipitation data

CWD

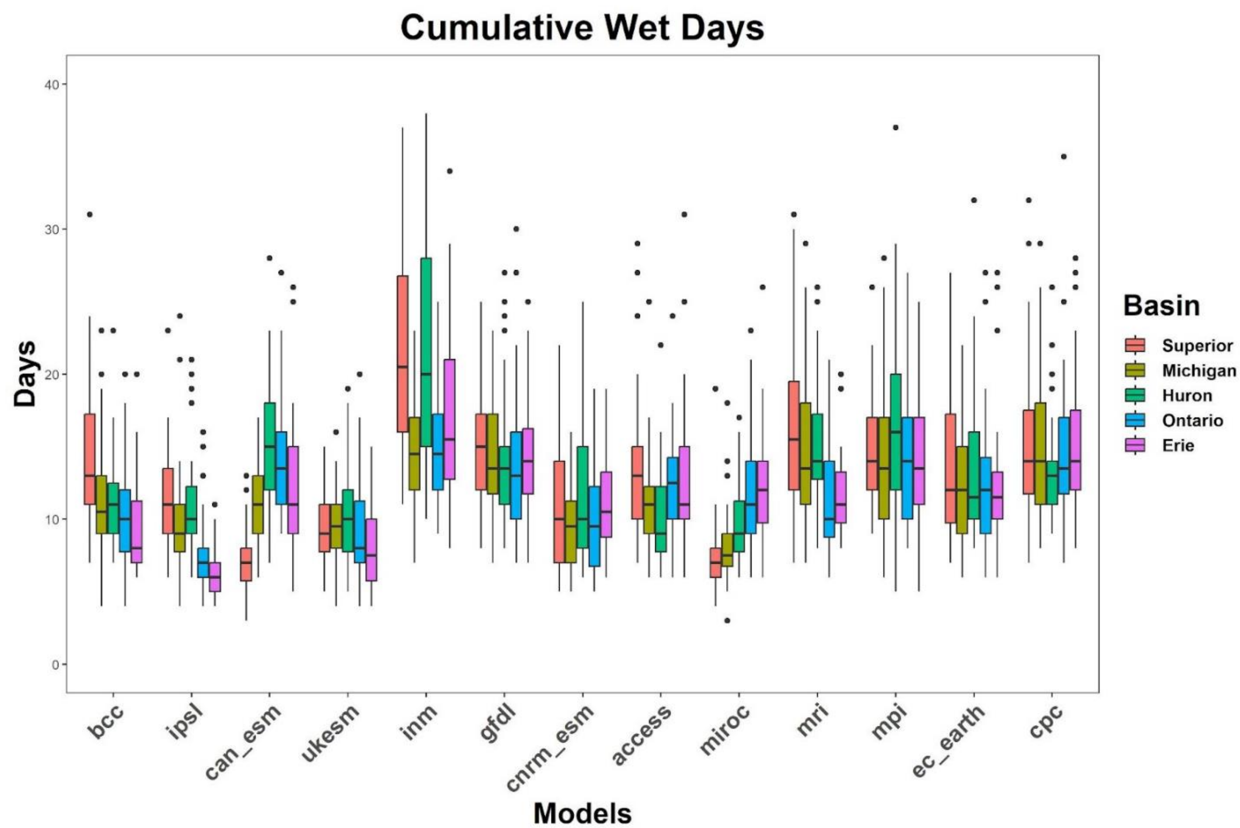

S4 : Same as S1 but for Cumulative Wet Days. Models in x-axis are arranged from higher to lower MVI values

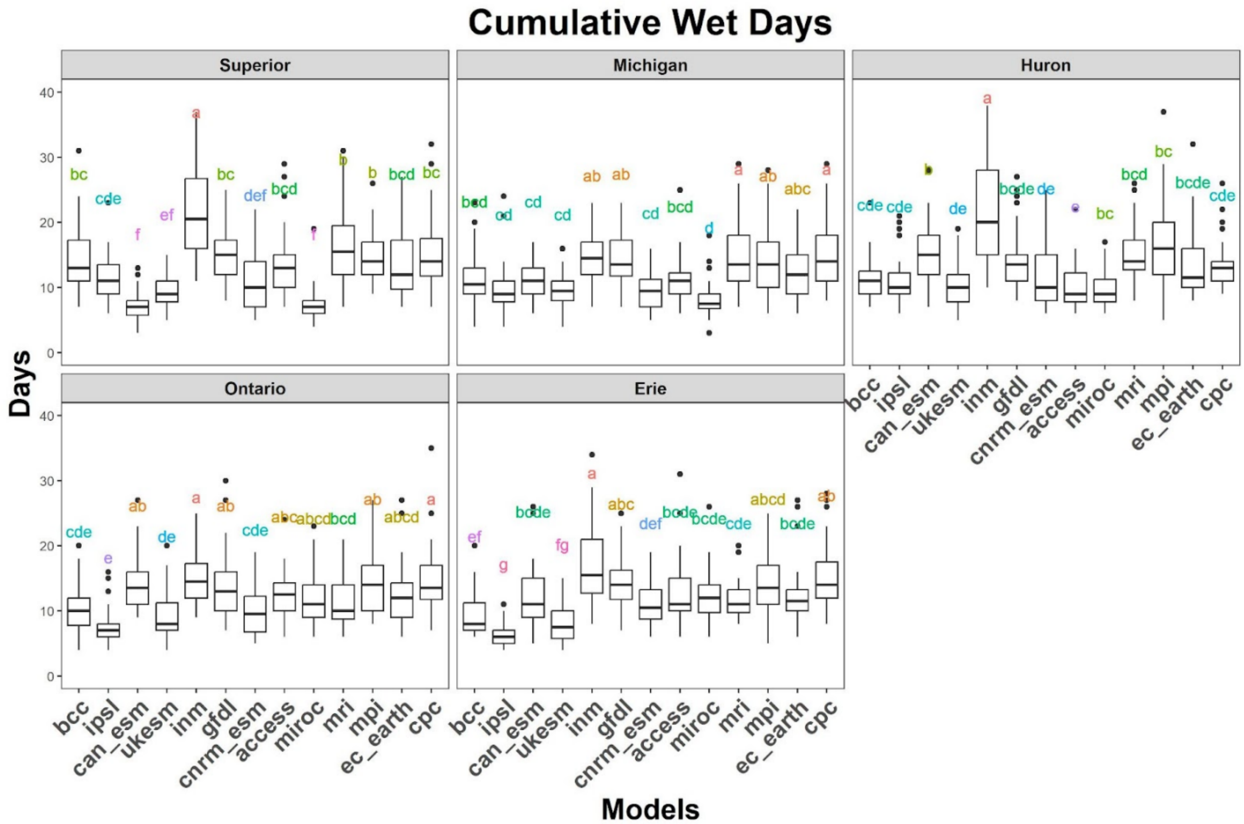

S5 : Same as S2 but for Cumulative Wet Days

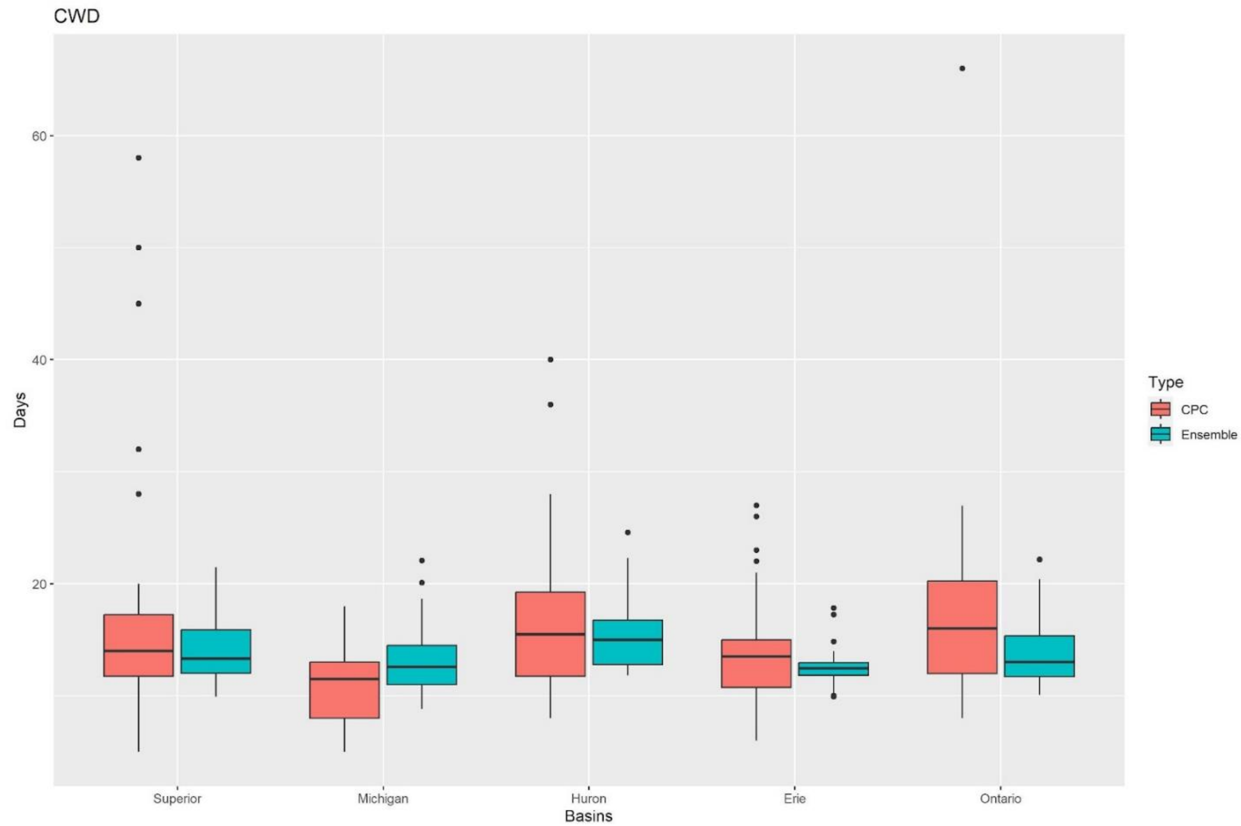

S6: Same as S3 but for Cumulative Wet Days

EPD

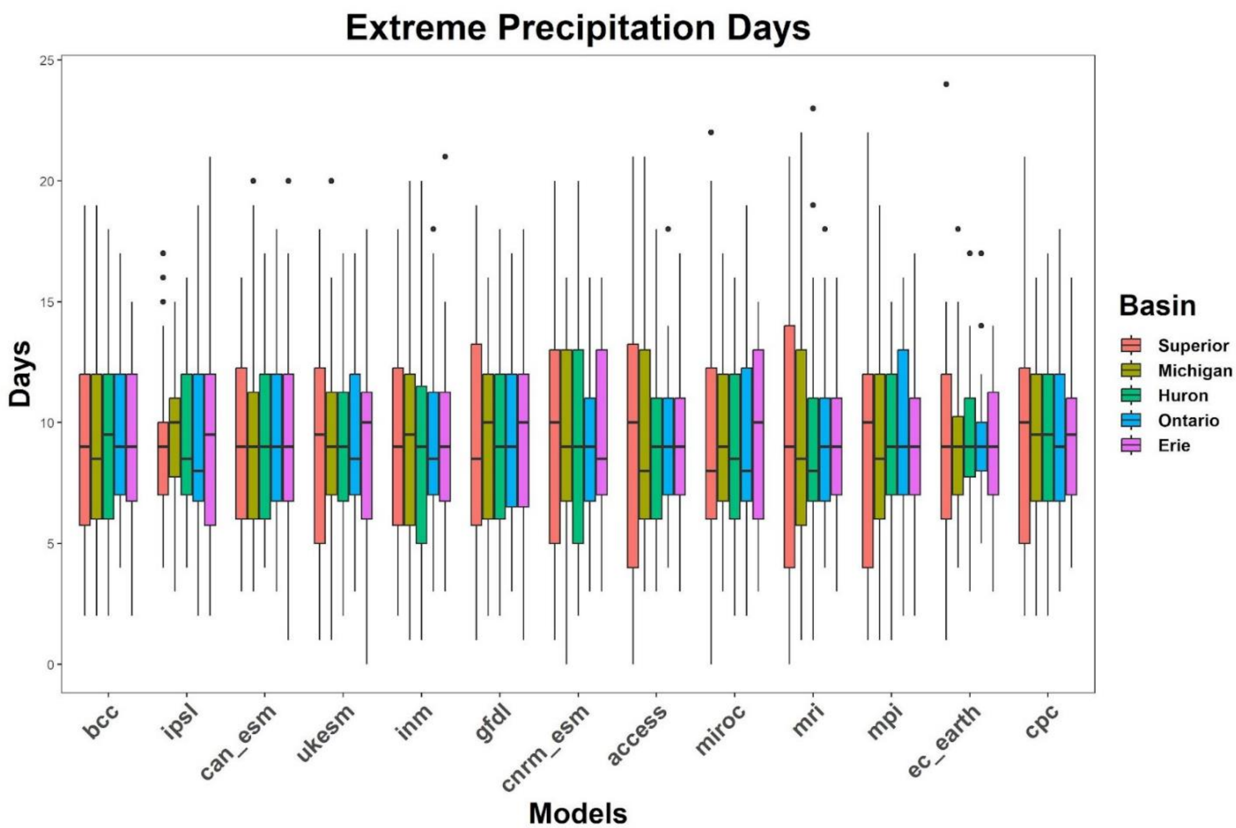

S7: Same as S1 but for Extreme Precipitation Days

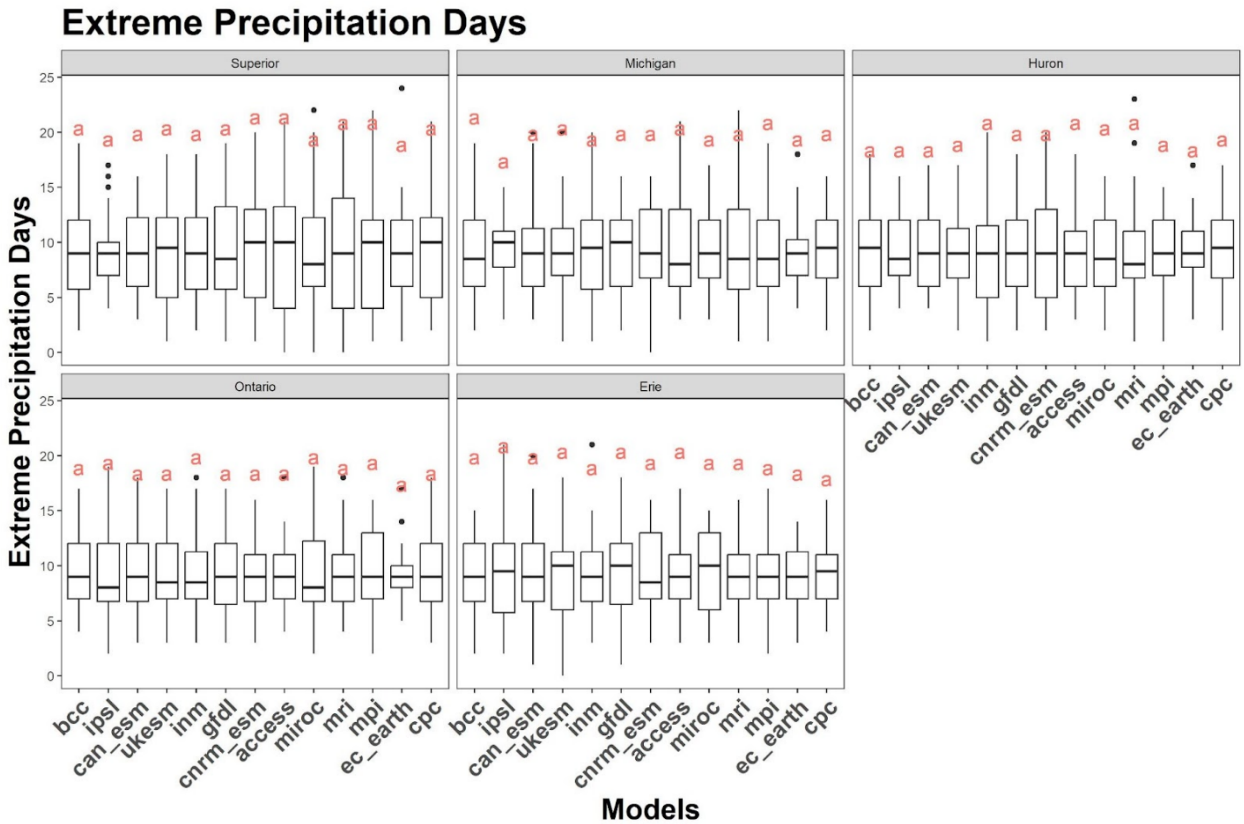

S8: Same as S2 but for Extreme Precipitation Days

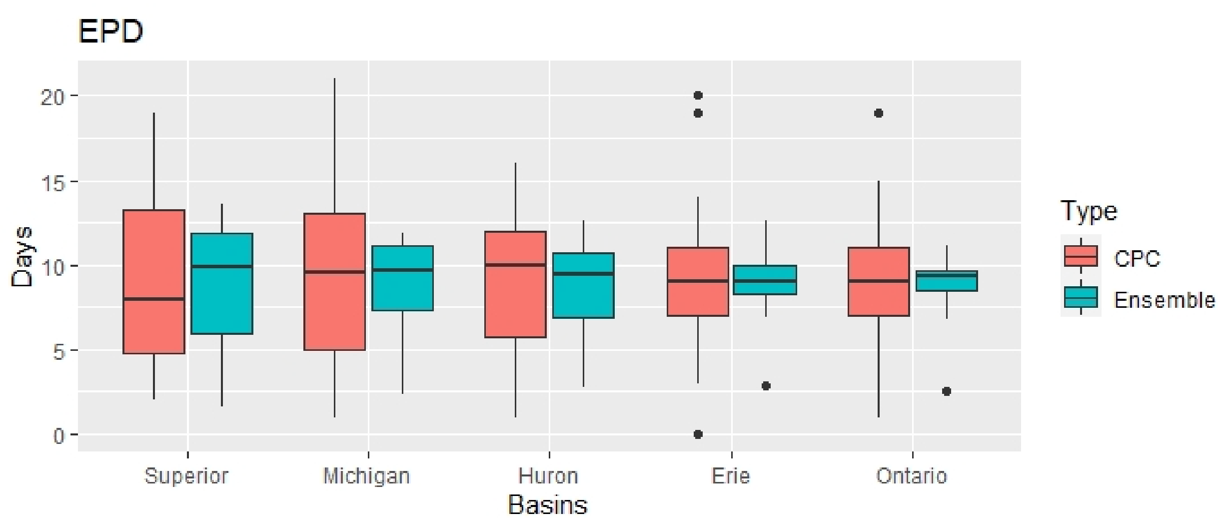

S9: Same as S3 but for Extreme Precipitation Days

MDP

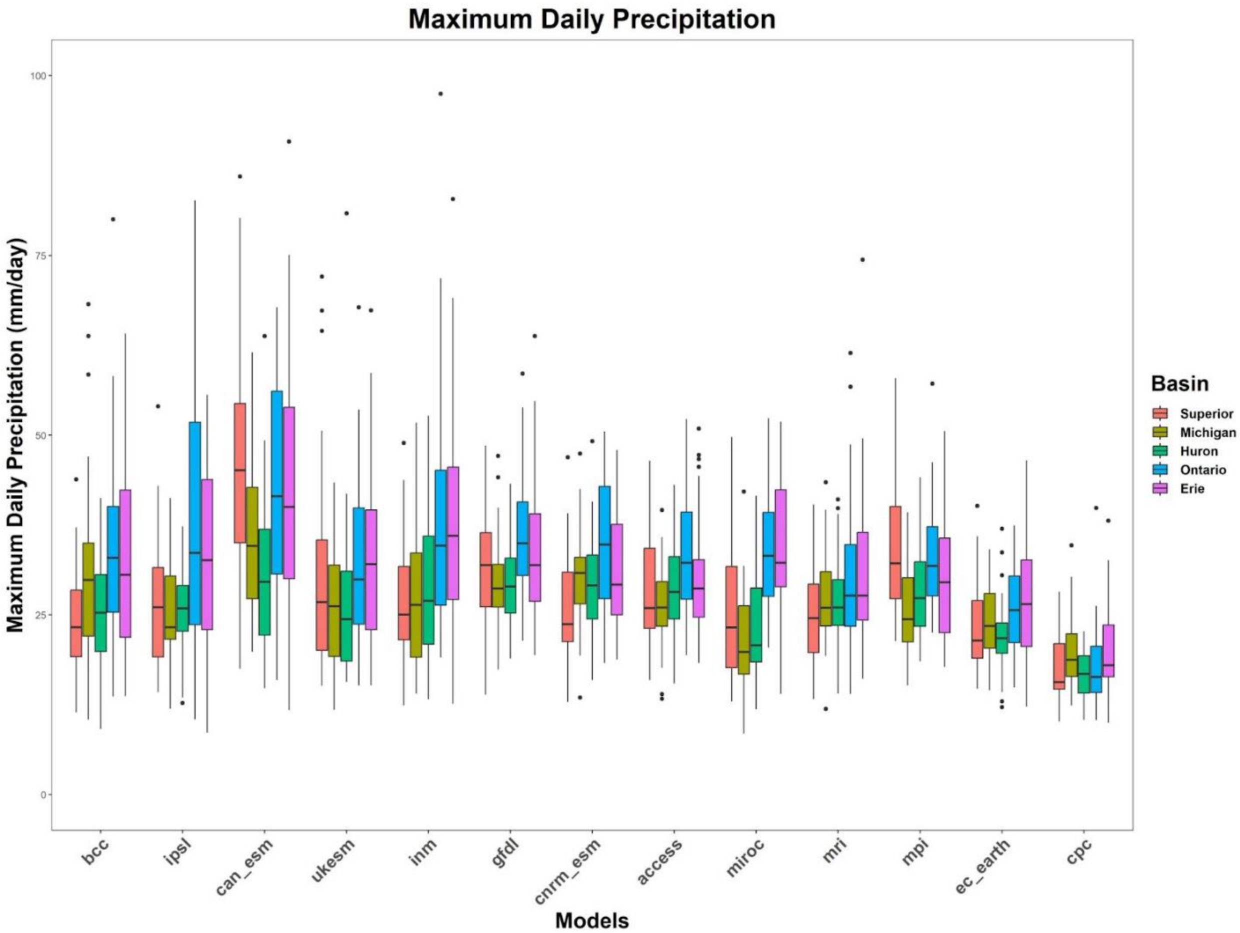

S10: Same as S1 but for Maximum Daily Precipitation

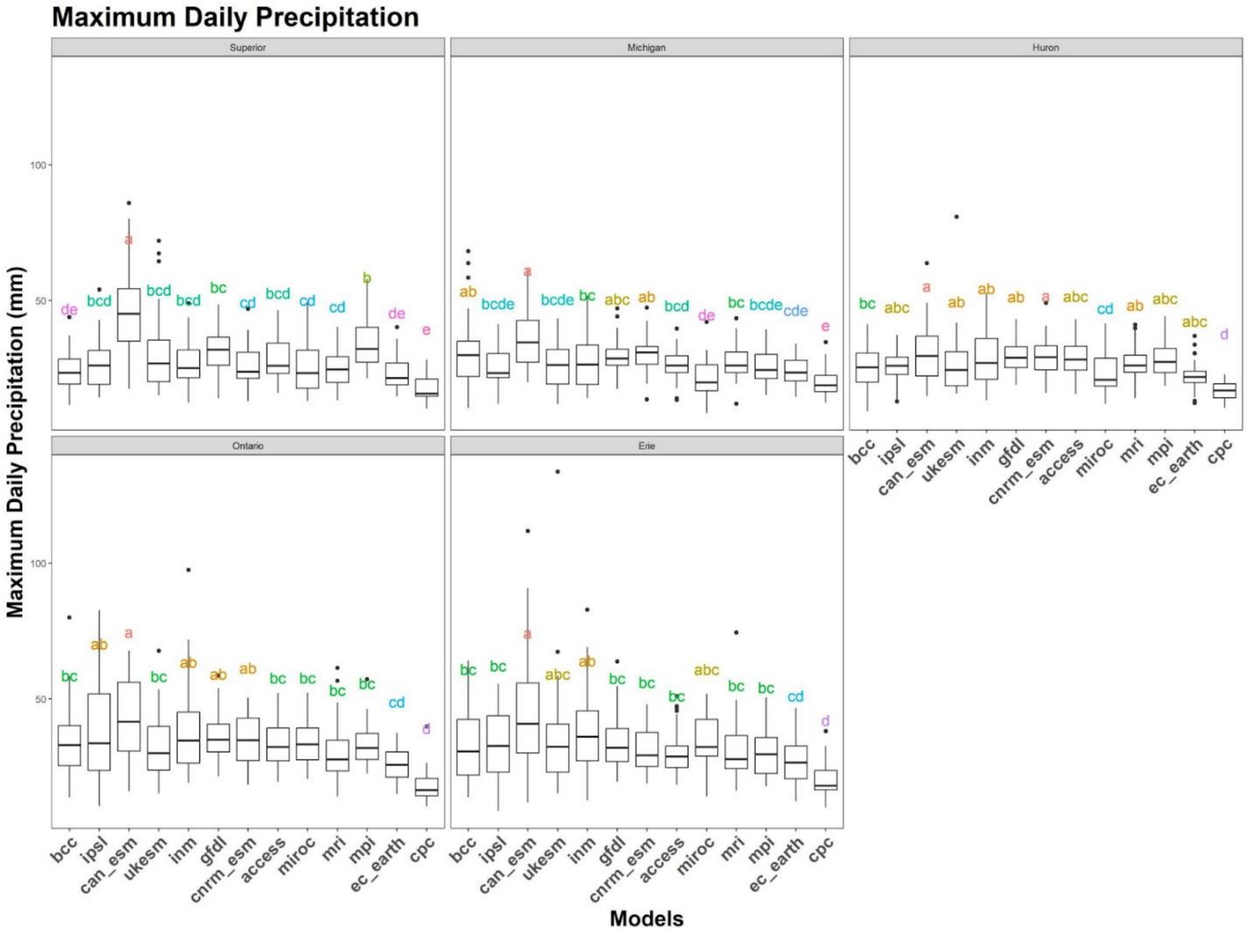

S11: Same as S2 but for Maximum Daily Precipitation

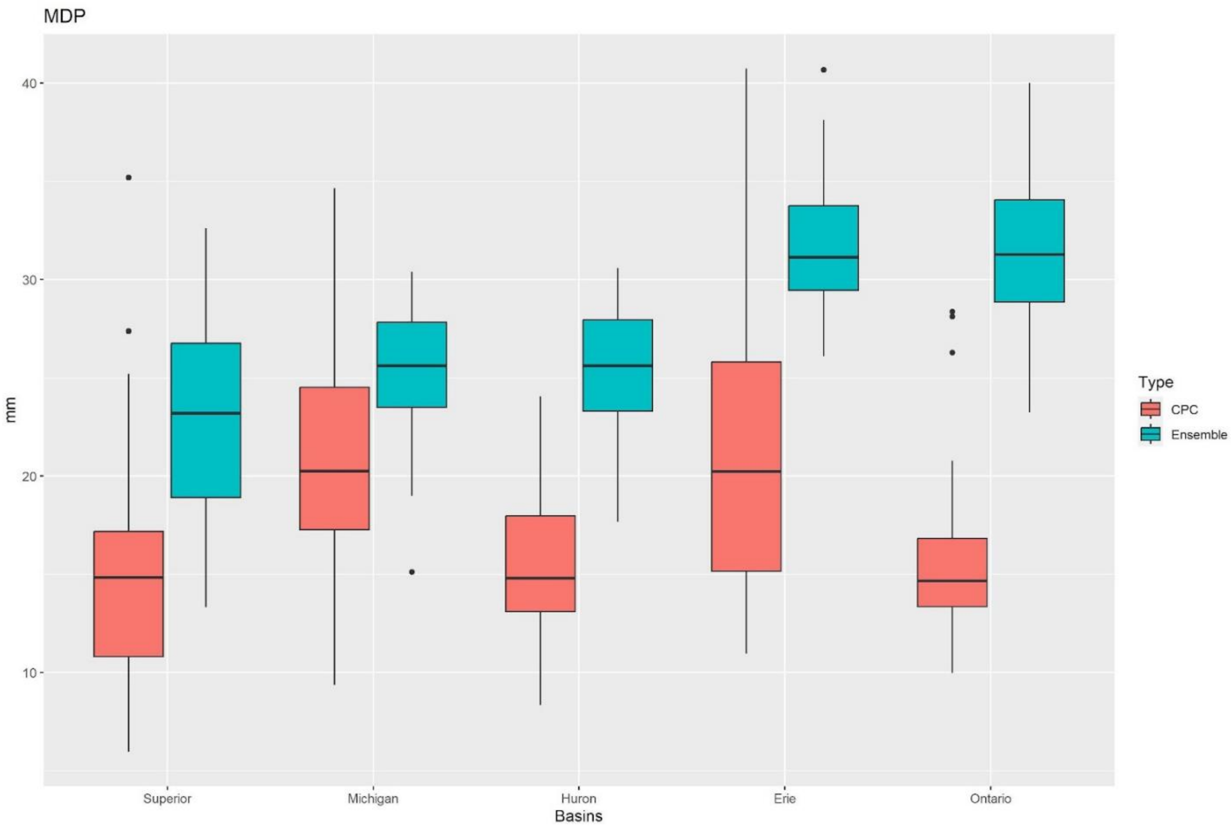

S12: Same as S3 but for Maximum Daily Precipitation

TP

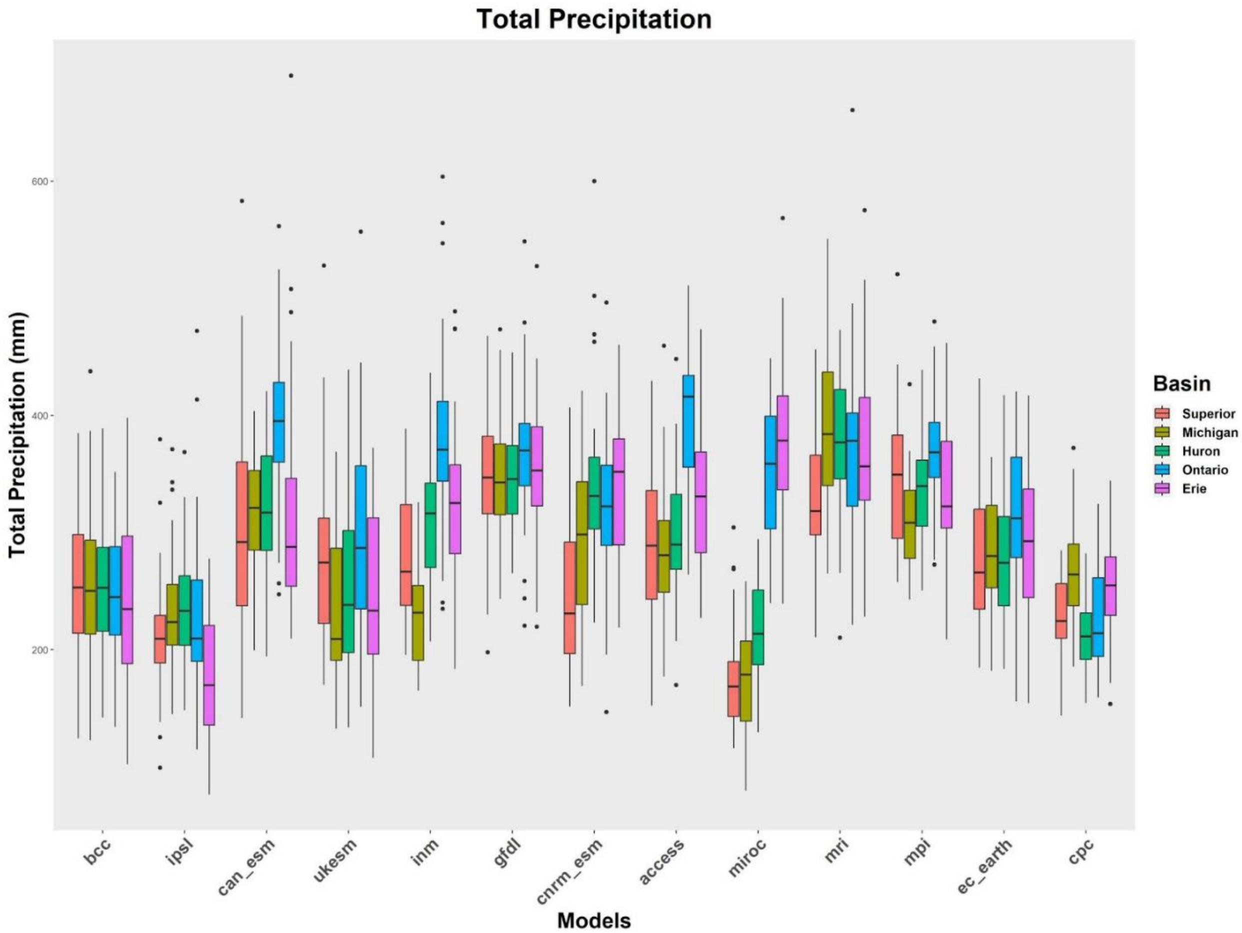

S13: Same as S1 but for Total Precipitation

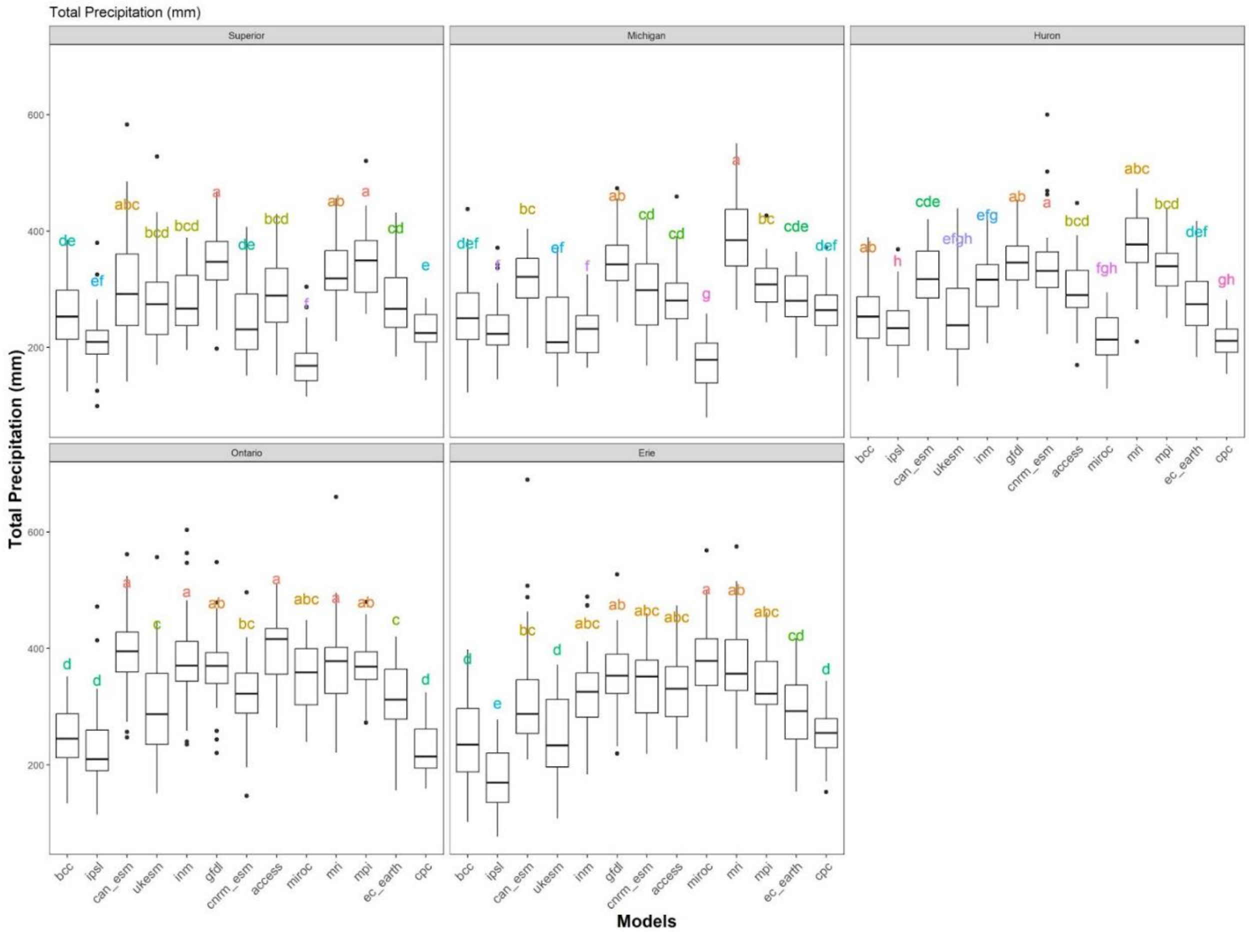

S14: Same as S2 but for Total Precipitation

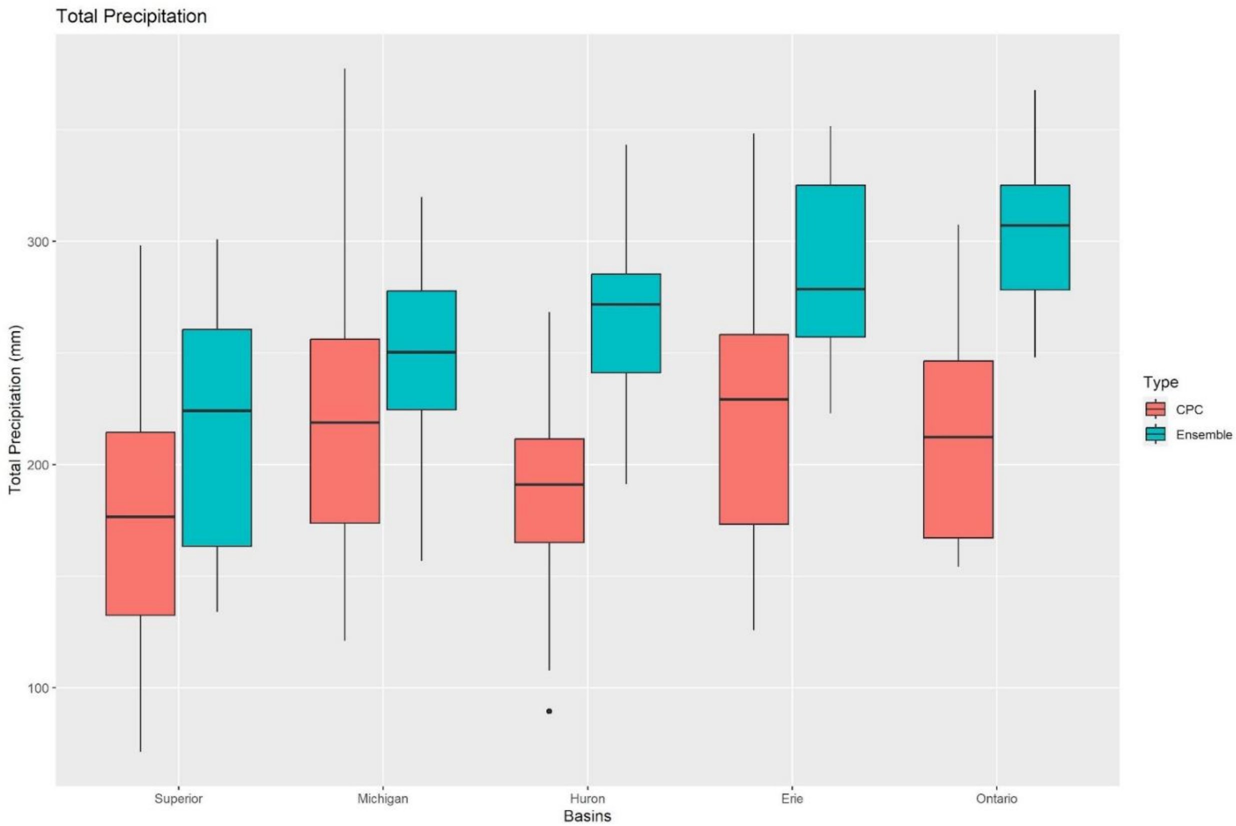

S15: Same as S3 but for Total Precipitation

Section 7: REFERENCES

Agel, L., Barlow, M., Feldstein, S.B. et al. Identification of large-scale meteorological patterns associated with extreme precipitation in the US northeast. Clim Dyn 50, 1819–1839 (2018). https://doi.org/10.1007/s00382-017-3724-8

Agel, L., and M. Barlow, 2020: How Well Do CMIP6 Historical Runs Match Observed Northeast U.S. Precipitation and Extreme Precipitation–Related Circulation? J. Climate, 33, 9835–9848, https://doi.org/10.1175/JCLI-D-19-1025.1.

Akinsanola, A. A., G. J. Kooperman, K. A. Reed, A. G. Pendergrass, and W. M. Hannah. 2020. “Projected Changes in Seasonal Precipitation Extremes over the United States in CMIP6 Simulations.” Environmental Research Letters. https://doi.org/10.1088/1748-9326/abb397.

Allen, M., Ingram, W. Constraints on future changes in climate and the hydrologic cycle. Nature 419, 224–232 (2002).

https://doi.org/10.1038/nature01092

Amal John, Hervé Douville, Aurélien Ribes, Pascal Yiou,Quantifying CMIP6 model uncertainties in extreme precipitation projections, Weather and Climate Extremes, Volume 36,2022, 100435,ISSN 2212-0947,

https://doi.org/10.1016/j.wace.2022.100435.

Boucher, Olivier; Denvil, Sébastien; Levavasseur, Guillaume; Cozic, Anne; Caubel, Arnaud; Foujols, Marie-Alice; Meurdesoif, Yann; Cadule, Patricia; Devilliers, Marion; Ghattas, Josefine; Lebas, Nicolas; Lurton, Thibaut; Mellul, Lidia; Musat, Ionela; Mignot, Juliette; Cheruy, Frédérique (2018). IPSL IPSL-CM6A-LR model output prepared for CMIP6 CMIP historical. Version YYYYMMDD[1].Earth System Grid Federation.

https://doi.org/10.22033/ESGF/CMIP6.5195

Cai, W., Borlace, S., Lengaigne, M. et al. Increasing frequency of extreme El Niño events due to greenhouse warming. Nature Clim Change 4, 111–116 (2014).
https://doi.org/10.1038/nclimate2100

CanESM5 model output prepared for CMIP6 CMIP historical. Version YYYYMMDD[1].Earth System Grid Federation.

https://doi.org/10.22033/ESGF/CMIP6.3610

Carter, E., & Steinschneider, S. (2018). Hydroclimatological drivers of extreme floods on Lake Ontario. Water Resources Research, 54, 4461– 4478.

https://doi.org/10.1029/2018WR022908

Carter, E., D. A. Herrera, and S. Steinschneider, 2021: Feature Engineering for Subseasonal-to-Seasonal Warm-Season Precipitation Forecasts in the Midwestern United States: Toward a Unifying Hypothesis of Anomalous Warm-Season Hydroclimatic Circulation. J. Climate, 34, 8291–8318,

https://doi.org/10.1175/JCLI-D-20-0264.1.

Chen, M., Shi, W., Xie, P., Silva, V. B. S., Kousky, V. E., Wayne Higgins, R., and Janowiak, J. E. (2008), Assessing objective techniques for gauge-based analyses of global daily precipitation, J. Geophys. Res., 113, D04110,

https://doi:10.1029/2007JD009132.

Chen, W., Z. Jiang, and L. Li, 2011: Probabilistic Projections of Climate Change over China under the SRES A1B Scenario Using 28 AOGCMs. J. Climate, 24, 4741–4756, https://doi.org/10.1175/2011JCLI4102.1.

Chen, L., T. W. Ford, and E. Swenson, 2023: The Role of the Circulation Patterns in Projected Changes in Spring and Summer Precipitation Extremes in the U.S. Midwest. J. Climate, 36, 1943–1956,

https://doi.org/10.1175/JCLI-D-22-0245.1.

Dai, A., and K. E. Trenberth, 2004: The Diurnal Cycle and Its Depiction in the Community Climate System Model. J. Climate, 17, 930–951, https://doi.org/10.1175/1520-0442(2004)017<0930:TDCAID>2.0.CO;2

David J; Ploshay, Jeffrey; Reichl, Brandon G; Schwarzkopf, Daniel M; Seman, Charles J; Silvers, Levi; Wyman, Bruce; Zeng, Yujin; Adcroft, Alistair; Dunne, John P.; Dussin, Raphael; Guo, Huan; He, Jian; Held, Isaac M; Horowitz, Larry W.; Lin, Pu; Milly, P.C.D; Shevliakova, Elena; Stock, Charles; Winton, Michael; Wittenberg, Andrew T.; Xie, Yuanyu; Zhao, Ming (2018). NOAA-GFDL GFDL-ESM4 model output prepared for CMIP6 CMIP historical. Version YYYYMMDD[1].Earth System Grid Federation. https://doi.org/10.22033/ESGF/CMIP6.8597

D'Orgeville M, Peltier WR, Erler AR, Gula J (2014) Climate change impacts on Great Lakes Basin precipitation extremes. J Geophys Res: Atmos 119(18):10799–710812 https://doi.org/10.1002/2014JD021855

Dollan, Ishrat Jahan, Viviana Maggioni, Jeremy Johnston, Gustavo de A. Coelho, and James L. Kinter. 2022. "Seasonal Variability of Future Extreme Precipitation and Associated Trends across the Contiguous U.S." Frontiers in Climate. https://doi.org/10.3389/fclim.2022.954892.

EC-Earth Consortium (EC-Earth) (2019). EC-Earth-Consortium EC-Earth3 model output prepared for CMIP6 CMIP historical. Version YYYYMMDD[1].Earth System Grid Federation.

https://doi.org/10.22033/ESGF/CMIP6.4700

Eyring, Veronika, Sandrine Bony, Gerald A. Meehl, Catherine A. Senior, Bjorn Stevens, Ronald J. Stouffer, and Karl E. Taylor. 2016. "Overview of the Coupled Model Intercomparison Project Phase 6 (CMIP6) Experimental Design and Organization." Geoscientific Model Development 9 (5): 1937–58

https://doi.org/10.5194/gmd-9-1937-2016

Gibson, P. B., D. E. Waliser, H. Lee, B. Tian, and E. Massoud, 2019: Climate Model Evaluation in the Presence of Observational Uncertainty: Precipitation Indices over the Contiguous United States. J. Hydrometeor., 20, 1339–1357,

https://doi.org/10.1175/JHM-D-18-0230.1.

Gimeno, L., Drumond, A., Nieto, R., Trigo, R. M., and Stohl, A. (2010), On the origin of continental precipitation, Geophys. Res. Lett., 37, L13804,

https://doi.org/10.1029/2010GL043712

Hajima, Tomohiro; Abe, Manabu; Arakawa, Osamu; Suzuki, Tatsuo; Komuro, Yoshiki; Ogura, Tomoo; Ogochi, Koji; Watanabe, Michio; Yamamoto, Akitomo; Tatebe, Hiroaki; Noguchi, Maki A.; Ohgaito, Rumi; Ito, Akinori; Yamazaki, Dai; Ito, Akihiko; Takata, Kumiko; Watanabe, Shingo; Kawamiya, Michio; Tachiiri, Kaoru (2019). MIROC MIROC-ES2L model output prepared for CMIP6 CMIP historical. Version YYYYMMDD[1].Earth System Grid Federation.

https://doi.org/10.22033/ESGF/CMIP6.5602

Jiang, Z., W. Li, J. Xu, and L. Li, 2015: Extreme Precipitation Indices over China in CMIP5 Models. Part I: Model Evaluation. J. Climate, 28, 8603–8619,

https://doi.org/10.1175/JCLI-D-15-0099.1

Kalnay, E., and Coauthors, 1996: The NCEP/NCAR 40-Year Reanalysis Project. Bull. Amer. Meteor. Soc., 77, 437–472,

https://doi.org/10.1175/1520-0477(1996)077<0437:TNYRP>2.0.CO;2.

Krasting, John P.; John, Jasmin G; Blanton, Chris; McHugh, Colleen; Nikonov, Serguei; Radhakrishnan, Aparna; Rand, Kristopher; Zadeh, Niki T.; Balaji, V; Durachta, Jeff; Dupuis, Christopher; Menzel, Raymond; Robinson, Thomas; Underwood, Seth; Vahlenkamp, Hans; Dunne, Krista A.; Gauthier, Paul PG; Ginoux, Paul; Griffies, Stephen M.; Hallberg, Robert; Harrison, Matthew; Hurlin, William; Malyshev, Sergey; Naik, Vaishali; Paulot, Fabien; Paynter, Volodin, Evgeny; Mortikov, Evgeny; Gritsun, Andrey; Lykossov, Vasily; Galin, Vener; Diansky, Nikolay; Gusev, Anatoly; Kostrykin, Sergey; Iakovlev, Nikolay; Shestakova, Anna;

Emelina, Svetlana (2019). INM INM-CM5-0 model output prepared for CMIP6 CMIP historical. Version YYYYMMDD[1].Earth System Grid Federation.

https://doi.org/10.22033/ESGF/CMIP6.5070

Labe, Z., Ault, T. & Zurita-Milla, R. Identifying anomalously early spring onsets in the CESM large ensemble project. Clim Dyn 48, 3949–3966 (2017).

https://doi.org/10.1007/s00382-016-3313-2

Laura J. Briley, Richard B. Rood, Michael Notaro,Large lakes in climate models: A Great Lakes case study on the usability of CMIP5, Journal of Great Lakes Research,Volume 47, Issue 2, 2021,

https://doi.org/10.1016/j.jglr.2021.01.010.

Li, C., Sinha, E., Horton, D. E., Diffenbaugh, N. S., and Michalak, A. M. (2014), Joint bias correction of temperature and precipitation in climate model simulations, J. Geophys. Res. Atmos., 119, 13,153– 13,162,

https://doi.org/10.1002/2014JD022514

Li, C., F. Zwiers, X. Zhang, G. Li, Y. Sun, and M. Wehner, 2021: Changes in Annual Extremes of Daily Temperature and Precipitation in CMIP6 Models. J. Climate, 34, 3441–3460, https://doi.org/10.1175/JCLI-D-19-1013.1.

Liu, Lin, and Bruno Basso. 2020. "Impacts of Climate Variability and Adaptation Strategies on Crop Yields and Soil Organic Carbon in the US Midwest." PloS One 15 (1): e0225433. https://doi.org/10.1371/journal.pone.0225433

Li, W., L. Li, R. Fu, Y. Deng, and H. Wang, 2011: Changes to the North Atlantic Subtropical High and Its Role in the Intensification of Summer Rainfall Variability in the Southeastern United States. J. Climate, 24, 1499–1506, https://doi.org/10.1175/2010JCLI3829.1.

Li, X., Zhong, S., Bian, X., Heilman, W. E., Luo, Y., and Dong, W. (2010), Hydroclimate and variability in the Great Lakes region as derived from the North American Regional Reanalysis, J. Geophys. Res., 115, D12104, https://doi.org/10.1029/2009JD012756

Mailhot, E., Music, B., Nadeau, D.F. et al. Assessment of the Laurentian Great Lakes' hydrological conditions in a changing climate. Climatic Change 157, 243–259 (2019). https://doi.org/10.1007/s10584-019-02530-6

Mahony, Colin R., Tongli Wang, Andreas Hamann, and Alex J. Cannon. 2022. "A Global Climate Model Ensemble for Downscaled Monthly Climate Normals over North America." International Journal of Climatology, March.

https://doi.org/10.1002/joc.7566.

May H, Rixon S, Gardner S, Goel P, Levison J, Binns A. Investigating relationships between climate controls and nutrient flux in surface waters, sediments, and subsurface pathways in an agricultural clay catchment of the Great Lakes Basin. Sci Total Environ. 2023 Mar 15;864:160979. doi: 10.1016/j.scitotenv.2022.160979. Epub 2022 Dec 20. PMID: 36549520.

https://doi.org/10.1016/j.scitotenv.2022.160979

Minallah, S., and A. L. Steiner, 2021: Role of the Atmospheric Moisture Budget in Defining the Precipitation Seasonality of the Great Lakes Region. J. Climate, 34, 643–657, https://doi.org/10.1175/JCLI-D-19-0952.1.

Minallah, S. and A.L. Steiner (2021b) Analysis of the atmospheric water cycle for the Laurentian Great Lakes region using CMIP6 models, Journal of Climate, 34, 12, 4693-4710, https://doi.org/10.1029/2009JD012756

Neubauer, David; Ferrachat, Sylvaine; Siegenthaler-Le Drian, Colombe; Stoll, Jens; Folini, Doris Sylvia; Tegen, Ina; Wieners, Karl-Hermann; Mauritsen, Thorsten; Stemmler, Irene; Barthel, Stefan; Bey, Isabelle; Daskalakis, Nikos; Heinold, Bernd; Kokkola, Harri; Partridge, Daniel; Rast, Sebastian; Schmidt, Hauke; Schutgens, Nick; Stanelle, Tanja; Stier, Philip; Watson-Parris, Duncan; Lohmann, Ulrike (2019). HAMMOZ-Consortium MPI-ESM1.2-HAM model output prepared for CMIP6 CMIP historical. Version YYYYMMDD[1].Earth System Grid Federation.

https://doi.org/10.22033/ESGF/CMIP6.5016

Nijsse, F. J. M. M., Cox, P. M., and Williamson, M. S.: Emergent constraints on transient climate response (TCR) and equilibrium climate sensitivity (ECS) from historical warming in CMIP5 and CMIP6 models, Earth Syst. Dynamics., 11, 737–750,

https://doi.org/10.5194/esd-11-737-2020, 2020.

NOAA's Climate Prediction Center. 2001. "NOAA's Climate Prediction Center," January. https://origin.cpc.ncep.noaa.gov/products/analysis_monitoring/ensostuff/ONI_v5.php.

Paxton Andrew, Schoof Justin T., Ford Trent W., Remo Jonathan W. F. Extreme Precipitation in the Great Lakes Region: Trend Estimation and Relation With Large-Scale Circulation and Humidity,Frontiers in Water ,3,2021,

https://www.frontiersin.org/articles/10.3389/frwa.2021.782847

Peltier, W. R., M. D'Orgeville, A. R. Erler, and F. Xie, 2018: Uncertainty in Future Summer Precipitation in the Laurentian Great Lakes Basin: Dynamical Downscaling and the Influence of Continental-Scale Processes on Regional Climate Change. J. Climate, 31, 2651–2673,

https://doi.org/10.1175/JCLI-D-17-0416.1.

Pendergrass, A. G., and D. L. Hartmann, 2014: The Atmospheric Energy Constraint on Global-Mean Precipitation Change. J. Climate, 27, 757–768,

https://doi.org/10.1175/JCLI-D-13-00163.1.

Pendergrass, Angeline G., Flavio Lehner, Benjamin M. Sanderson, and Yangyang Xu. 2015. "Does Extreme Precipitation Intensity Depend on the Emissions Scenario?" Geophysical Research Letters.

https://doi.org/10.1002/2015gl065854.

Peter; Mackallah, Chloe; Sullivan, Arnold; O'Farrell, Siobhan; Druken, Kelsey (2019). CSIRO ACCESS-ESM1.5 model output prepared for CMIP6 CMIP historical. Version YYYYMMDD[1].Earth System Grid Federation.
https://doi.org/10.22033/ESGF/CMIP6.4272

Pfahl, S., O'Gorman, P. & Fischer, E. Understanding the regional pattern of projected future changes in extreme precipitation. Nature Clim Change 7, 423–427(2017).
https://doi.org/10.1038/nclimate3287

Rey, D., Neuhäuser, M. (2011). Wilcoxon-Signed-Rank Test. In: Lovric, M. (eds) International Encyclopedia of Statistical Science. Springer, Berlin, Heidelberg.
https://doi.org/10.1007/978-3-642-04898-2_616

Rodionov, S. N., 1994: Association between Winter Precipitation and Water Level Fluctuations in the Great Lakes and Atmospheric Circulation Patterns. J. Climate, 7, 1693–1706,
https://doi.org/10.1175/1520-0442(1994)007<1693:ABWPAW>2.0.CO;2.

Seager, R., N. Naik, and G. A. Vecchi, 2010: Thermodynamic and Dynamic Mechanisms for Large-Scale Changes in the Hydrological Cycle in Response to Global Warming. J. Climate, 23, 4651–4668, https://doi.org/10.1175/2010JCLI3655.1

Seager, R., and Coauthors, 2014: Dynamical and Thermodynamical Causes of Large-Scale Changes in the Hydrological Cycle over North America in Response to Global Warming. J. Climate, 27, 7921–7948,

https://doi.org/10.1175/JCLI-D-14-00153.1.

Seager, R., and M. Hoerling, 2014: Atmosphere and Ocean Origins of North American Droughts. J. Climate, 27, 4581–4606,

https://doi.org/10.1175/JCLI-D-13-00329.1.

Seferian, Roland (2018). CNRM-CERFACS CNRM-ESM2-1 model output prepared for CMIP6 CMIP historical. Version YYYYMMDD[1].Earth System Grid Federation.

https://doi.org/10.22033/ESGF/CMIP6.4068

Shrestha, Narayan K., Frank Seglenieks, André G. T. Temgoua, and Armin Dehghan. 2022.“The Impacts of Climate Change on Land Hydroclimatology of the Laurentian Great Lakes Basin.” Frontiers in Water 4 (July).

https://doi.org/10.3389/frwa.2022.801134

Steinschneider, S., McCrary, R., Mearns, L. O., and Brown, C. (2015), The effects of climate model similarity on probabilistic climate projections and the implications for local, risk-based adaptation planning. Geophys. Res. Lett., 42, 5014– 5044.

https://doi.org/10.1002/2015GL064529

Swart, Neil Cameron; Cole, Jason N.S.; Kharin, Viatcheslav V.; Lazare, Mike; Scinocca, John F.; Gillett, Nathan P.; Anstey, James; Arora, Vivek; Christian, James R.; Jiao, Yanjun; Lee, Warren G.; Majaess, Fouad; Saenko, Oleg A.; Seiler, Christian; Seinen, Clint; Shao, Andrew; Solheim, Larry; von Salzen, Knut; Yang, Duo; Winter, Barbara; Sigmond, Michael (2019). CCCma CanESM5 model output prepared for CMIP6 CMIP historical. Version YYYYMMDD[1].Earth System Grid Federation.

https://doi.org/10.22033/ESGF/CMIP6.3610

Srivastava Abhishek, Richard Grotjahn, Paul A. Ullrich, Evaluation of historical CMIP6 model simulations of extreme precipitation over contiguous US regions, Weather and Climate Extremes, Volume 29,2020, 100268, ISSN 2212-0947,

https://doi.org/10.1016/j.wace.2020.100268**.**

Tokarska, Katarzyna B., Martin B. Stolpe, Sebastian Sippel, Erich M. Fischer, Christopher J.Smith, Flavio Lehner, and Reto Knutti. 2020. "Past Warming Trend Constraints Future

Warming in CMIP6 Models." Science Advances 6 (12): eaaz9549.

https://doi.org/10.1126/sciadv.aaz9549

Trenberth, K.E. (1999). Conceptual Framework for Changes of Extremes of the Hydrological Cycle with Climate Change. In: Karl, T.R., Nicholls, N., Ghazi, A. (eds) Weather and Climate Extremes. Springer, Dordrecht.

https://doi.org/10.1007/978-94-015-9265-9_18

Trenberth KE (2011) Changes in Precipitation with Climate Change. Clim Res 47:123-138.

https://doi: 10.3354/cr00953

Wang, D., Chen, Y., Jarin, M. et al. Increasingly frequent extreme weather events urge the development of point-of-use water treatment systems. npj Clean Water 5, 36 (2022).

https://doi.org/10.1038/s41545-022-00182-1

Wang, Tongli, Andreas Hamann, Dave Spittlehouse, and Carlos Carroll. 2016. "Locally Downscaled and Spatially Customizable Climate Data for Historical and Future Periods for North America." PloS One 11 (6): e0156720.

https://doi.org/10.1371/journal.pone.0156720

Wu, Tongwen; Chu, Min; Dong, Min; Fang, Yongjie; Jie, Weihua; Li, Jianglong; Li, Weiping; Liu, Qianxia; Shi, Xueli; Xin, Xiaoge; Yan, Jinghui; Zhang, Fang; Zhang, Jie; Zhang, Li; Zhang, Yanwu (2018). BCC BCC-CSM2MR model output prepared for CMIP6 CMIP historical. Version YYYYMMDD[1].Earth System Grid Federation.
https://doi.org/10.22033/ESGF/CMIP6.2948

Yukimoto, Seiji; Koshiro, Tsuyoshi; Kawai, Hideaki; Oshima, Naga; Yoshida, Kohei. Urakawa, Shogo; Tsujino, Hiroyuki; Deushi, Makoto; Tanaka, Taichu; Hosaka, Masahiro, Yoshimura, Hiromasa; Shindo, Eiki; Mizuta, Ryo; Ishii, Masayoshi; Obata, Atsushi, Adachi, Yukimasa (2019). MRI MRI-ESM2.0 model output prepared for CMIP6 CMIP historical. Version YYYYMMDD[1].Earth System Grid Federation.
https://doi.org/10.22033/ESGF/CMIP6.6842

Zhang, X., Alexander, L., Hegerl, G.C., Jones, P., Tank, A.K., Peterson, T.C., Trewin, B. and Zwiers, F.W. (2011), Indices for monitoring changes in extremes based on daily temperature and precipitation data. WIREs Clim Change, 2: 851-870.
https://doi.org/10.1002/wcc.147

Zhou, W., L. R. Leung, and J. Lu, 2022: Seasonally Dependent Future Changes in the U.S. Midwest Hydroclimate and Extremes. J. Climate, 35, 17–27, https://doi.org/10.1175/JCLI-D-21-0012.1.

Ziehn, Tilo; Chamberlain, Matthew; Lenton, Andrew; Law, Rachel; Bodman, Roger; Dix, Martin; Wang, Yingping; Dobrohotoff, Peter; Srbinovsky, Jhan; Stevens, Lauren; Vohralik, Peter; Mackallah, Chloe; Sullivan, Arnold; O'Farrell, Siobhan; Druken, Kelsey (2019). CSIRO ACCESS-ESM1.5 model output prepared for CMIP6 CMIP historical. Version YYYYMMDD[1].Earth System Grid Federation. https://doi.org/10.22033/ESGF/CMIP6.4272eference

Zorzetto, E., and L. Li, 2021: Impacts of the North Atlantic Subtropical High on Daily Summer Precipitation over the Conterminous United States. J. Hydrometeor., 22, 1697–1712, https://doi.org/10.1175/JHM-D-20-0242.1.

Tasmeem Jahan Meem

315 Comstock Avenue, Syracuse, NY-13210

Phone: +1 (607) 262 6756, E-mail: tameem@syr.edu

Education

Syracuse University, Syracuse, NY
M.Sc. in Environmental Engineering (2021- Present)

Bangladesh University of Engineering and Technology, Dhaka, Bangladesh

B.Sc. in Chemical Engineering (2015-2019)

Professional Experience

Syracuse University, Syracuse, NY, USA

Graduate Research Assistant, Climate Hazards Research Lab Syracuse (Aug'22- Present)

Graduate Research Assistant, Climate Hazards Research Lab, Syracuse (Jan'21- Aug'21)

Deutsche Gesellschaft fur Internationale Zusammenarbeit GmBH(GIZ), Dhaka, Bangladesh

Junior Consultant, Promotion of Social and Environmental Standards in the Industries (Mar'20 – Jun'20)

Intern, Promotion of Social and Environmental Standards in the Industries (Sep'19 – Mar'20)

Poster Presentation

- **Meem, Tasmeem Jahan,** Carter, E.K., "Past and Future Hydro-climatologic Drivers of Precipitation Variability in the Great Lakes Region in CMIP6" – Frontiers in Hydrology Meeting 2022 at San Juan, Puerto Rico
- **Meem, Tasmeem Jahan,** Carter, E.K., "Past and Future Hydro-climatologic Drivers of Precipitation Variability in the Great Lakes Region in CMIP6" – AGU Fall Meeting 2022 at Chicago, IL, USA

Oral Presentation

- Islam,Md Tahmid & **Meem, Tasmeem Jahan**. "A Study on the Efficiency of Fatted and Defatted Moringa Oleifera Seed Extract (MOSE) on Indigo Carmine Dye Removal"- 3rd International Conference on Functional Materials and Chemical Engineering (ICFMCE 2019) at Chulalongkorn University, Bangkok, Thailand

Fellowships and Awards

- Syracuse University Fellowship (Sep'21 – Aug'22)
- AGU Travel Grant for Frontiers in Hydrology Meeting 2022, San Juan, Puerto Rico
- Nemerow Memorial Scholarship '22-23, Department of Civil and Environmental Engineering, Syracuse University
- Bangladesh Sweden Trust Fund Travel Grant, 2022

Professional Affiliation

- Member, American Geophysical Union (AGU)

Technical Skills

Programming: R, Python, MATLAB
Software: Git, Microsoft Visio, AQTESOLV, Aspen Hysys